The Novel Silver-Containing Antimicrobial Potentiates Aminoglycoside Activity Against *Pseudomonas aeruginosa.*

Gracious Yoofi Donkor[a], Greg M. Anderson[a], Michael Stadler[a], Patrick Ofori Tawiah[a], Carl D. Orellano[a], Kevin A. Edwards[b] and Jan-Ulrik Dahl[a#]

[a]School of Biological Sciences, Illinois State University, Microbiology, Normal, IL, USA

[b]School of Biological Sciences, Illinois State University, Cell Biology, Normal, IL, USA

RUNNING TITLE: Reactive oxygen species in antimicrobial therapy

[#]Address correspondence to Jan-Ulrik Dahl, email: jdahl1@ilstu.edu, phone: +1-(309)-438-7694

Word count:

Abstract: 248

Importance: 128

Manuscript:

Abstract

The rapid dissemination of antibiotic resistance combined with the decline in the discovery of novel antibiotics represents a major challenge for infectious disease control that can only be mitigated by investments into novel treatment strategies. Alternative antimicrobials including silver have regained interest due to their diverse mechanisms of inhibiting microbial growth. One such example is AGXX, a broad-spectrum antimicrobial that produces highly cytotoxic reactive oxygen species (ROS) to inflict extensive macromolecular damage. Due to connections identified between ROS production and antibiotic lethality, we hypothesized that AGXX could potentially increase the activity of conventional antibiotics. Using the gram-negative pathogen *Pseudomonas aeruginosa*, we screened possible synergistic effects of AGXX on several antibiotic classes. We found that the combination of AGXX and aminoglycosides tested at sublethal concentrations led to a rapid exponential decrease in bacterial survival and restored sensitivity of a kanamycin-resistant *P. aeruginosa* strain. We deciphered elevated ROS production as a significant contributor to the synergy and demonstrated that the addition of ROS scavengers resulted in reduced endogenous ROS levels and increased bacterial survival, while *P. aeruginosa* strains deficient in ROS detoxifying/repair genes were more susceptible to AGXX/aminoglycoside treatment. We further demonstrate that this synergistic interaction was associated with a significant increase in outer and inner membrane permeability, resulting in increased antibiotic influx. Our study also revealed that AGXX/aminoglycoside-mediated killing requires an active proton motive force across the bacterial membrane. Overall, our findings provide an understanding of cellular targets that could be inhibited to increase the activity of conventional antimicrobials.

IMPORTANCE

The emergence of drug-resistant bacteria coupled with the decline in antibiotic development highlights the need for novel alternatives. Thus, new strategies aimed at repurposing conventional antibiotics have gained significant interest. The necessity of these interventions is evident especially in gram-negative pathogens as they are

53 particularly difficult to treat due to their outer membrane. This study highlights the
54 effectiveness of the silver containing antimicrobial AGXX in potentiating aminoglycoside
55 activities against *P. aeruginosa*. The combination of AGXX and aminoglycosides not only
56 reduces bacterial survival rapidly but also significantly re-sensitizes aminoglycoside-
57 resistant strains. In combination with gentamicin, AGXX induces increased endogenous
58 oxidative stress, membrane damage and iron sulfur cluster disruption. These findings
59 emphasize AGXX's potential as a route of antibiotic adjuvant development and shed light
60 into potential targets to enhance aminoglycoside activity.

61

62 ## Introduction

63 The spread of antibiotic resistance has now reached a large number of bacterial
64 pathogens and evolved into a pertinent global health challenge (1). Over the past decade,
65 resistance has been reported against all classical antibiotics, including last resort
66 treatments such as polymyxins (2). The resistance crisis is further exacerbated in gram-
67 negative pathogens due to the impermeability of their outer membrane and the extensive
68 arsenal of drug resistance mechanisms that these critters employ. One example of a
69 difficult to treat gram-negative bacterium is the opportunistic pathogen *P. aeruginosa*, a
70 common cause of acute (e.g., wounds, burns) and chronic infections (e.g., diabetic ulcers,
71 cystic fibrosis) (3). *P. aeruginosa* is characterized by its high intrinsic and acquired
72 resistance mechanisms, allowing the pathogen to thrive in the presence of a large number
73 of antibiotics (4).

74 In light of these challenges, recent studies have focused on alternative treatment
75 strategies to limit bacterial infection and colonization (5, 6). Transition metals, such as
76 silver and copper, have long been recognized for their antimicrobial activities and were
77 already used by the ancient Greeks for would healing (7). Despite its long-standing history
78 and high efficiency against bacteria, the antimicrobial mode of action of silver is poorly
79 understood. Pleiotropic effects have been described and include changes in DNA
80 condensation, membrane alteration and protein damage (7, 8). Silver ions have a
81 particularly high affinity for cysteine thiols, disrupt exposed iron-sulfur clusters of

dehydratase enzymes, and replace metal-containing cofactors, thus affecting a wide range of cytoplasmic and membrane proteins (9, 10). More recently, silver derivates have received increased attention in medical applications, e.g. as antimicrobial surface-coatings on catheters and implants to protect against biofilm-forming bacteria and to reduce the risk of nosocomial infections (5, 11). One such promising silver-based antimicrobial with broad-spectrum activity is AGXX. AGXX consists of micro-galvanic elements of silver (Ag) and ruthenium (Ru), which are surface conditioned with ascorbic acid (12, 13). AGXX has been used in the form of a powder and implemented as an electroporated sheet on a variety of surfaces, including steel meshes, ceramics and water pipes, to limit bacterial colonization. AGXX's antimicrobial activity is not entirely dependent on the release of silver ions, but instead is proposed to occur through the generation of reactive oxygen species (ROS), such as hydroxyl radicals and superoxide (13–15). AGXX-generated ROS is produced through a series of redox reactions where the oxidized Ag component is reduced by organic matter and donates electrons to the valent Ru, which subsequently generates superoxide and other toxic ROS (12, 16). Previous studies revealed that, compared to classical silver and other metals, AGXX was significantly more bactericidal against gram-positive bacteria such as *Staphylococcus aureus* and *Enterococcus faecalis*, although no mechanistic details were provided (12, 13). Surprisingly, the antimicrobial effects of AGXX on gram-negative pathogens remain largely unexplored.

Compounds that generate ROS and/or stimulate endogenous oxidative stress in bacteria have gained interest as potential antibiotic adjuvants (17). Adjuvants increase the efficacy of antibiotics by targeting metabolic processes or cellular networks that ultimately lead to a synergistic increase in antibiotic potency (18). A classic example for the synergy between adjuvants and antibiotic is the combination of amoxicillin, a beta-lactam antibiotic, and clavulanic acid. Due to clavulanic acid's high affinity for beta-lactamase enzymes, its combination with the beta-lactam antibiotics, such as amoxicillin, synergistically potentiate their activity against penicillin-resistant bacteria (19). The hypothesis behind the synergistic effects of ROS-generating or -inducing compounds is based on the multimodal action of these compounds, which could potentially disrupt bacterial targets necessary for the defense of antibiotics (20). Recent studies on the

bactericidal mode of action of aminoglycoside, fluoroquinolone and beta-lactam antibiotics have proposed increased endogenous ROS stress as an additional mechanism for bacterial killing (5, 20, 21). Notably, activation of the bacterial envelope stress response, hyperactivation of the electron transport chain, and damage of iron sulfur clusters have been shown to contribute to an increase in endogenous ROS level (5). Although these findings are controversial, extensive evidence has been presented for the integral role of ROS-mediated damage in antibiotic-induced cell death (6). More importantly, recent studies employing ROS-generating compounds have reported promising results on their potential in sensitizing a wide variety of multidrug-resistant bacteria to both bactericidal and bacteriostatic antibiotics (5).

Given that AGXX's proposed mode of action is based on ROS production and studies with focus on evaluating potential synergistic effects of AGXX on conventional antibiotics are lacking, we started to investigate possible potentiating effects of AGXX on members of several antibiotic classes, using the *P. aeruginosa* strain PA14 as a model. Exploring potential synergies between AGXX and antibiotics could provide viable answers to the antimicrobial discovery drought, for instance by reducing the minimal inhibitory concentrations of conventional antibiotics required for treatment or possibly overriding and/or delaying antibiotic resistance development (22). By exposing PA14 to sublethal concentrations of AGXX and the antibiotics of interest alone and in combination, we found that bacterial survival was exponentially reduced when the cells were exposed to combinations of AGXX and aminoglycoside antibiotics. Moreover, combined treatment of both compounds re-sensitized a kanamycin resistant PA14 strain to sublethal concentrations of the antibiotic. We further demonstrate that the combined treatment of AGXX and aminoglycosides resulted in increased endogenous oxidative stress and a subsequent disruption of iron homeostasis, potentially providing an explanation for the elevated ROS level. The synergy was associated with a significant increase in outer and inner membrane permeability, which facilitates antibiotic influx. Moreover, our studies revealed that the synergy between AGXX and aminoglycosides relies on an active proton motive force across the bacterial membrane.

Results

AGXX is more efficient in killing *P. aeruginosa* than silverdene and silver nitrate. Studies with silver ions suggest that gram-negative bacteria are more susceptible than gram-positive bacteria (23). In this study, we investigated the effect of AGXX on *P. aeruginosa* using PA14 as model strain. To compare the effective antimicrobial concentrations of different AGXX formulations against PA14, we first performed survival analyses in the presence and absence of AGXX383, AGXX394, AGXX720C, and AGXX823, respectively. While these AGXX formulations all consist of the galvanized silver/ruthenium complex, they differ in various aspects such as silver ratio, particle size, and production procedure, which may affect their antimicrobial activity. Our time killing assays revealed that AGXX383 and AGXX394 have comparable antimicrobial activities against PA14 and are considerably more potent in inhibiting PA14 growth and survival compared to AGXX823 and AGXX720C (**Supplementary FIG S1**). Silver derivates have received increased attention in medical applications, e.g. as antimicrobial surface-coatings on catheters that protect from biofilm-forming bacteria and reduce the risk of nosocomial infections (24). Moreover, silver is used in topicals to prevent and/or treat infections in wounds (25). One such example is silver sulfadiazine (silverdene), the gold standard for treating and preventing *P. aeruginosa* infections in burn wound patients (26). However, silverdene is associated with complications such as allergic reactions to the sulfadiazine moiety emphasizing the need for novel treatment therapies (26). To compare the antimicrobial activities of AGXX394, silver nitrate and silverdene, we conducted survival studies of PA14 in the presence and absence of 25 μg/ml of each compound. Survival of PA14 was highly compromised when cells were exposed to AGXX394 (**Fig.1**). A direct comparison of the killing efficiencies between AGXX394 and silverdene and silver nitrate after 3 hours of treatment revealed a ~1-log and 2-log higher bactericidal activity for AGXX394, respectively, potentially making AGXX an attractive treatment/prevention alternative (**Fig. 1).**

AGXX exponentially increases the activity of aminoglycosides against P. aeruginosa. Our next goal was to determine whether inhibitors of DNA replication (fluoroquinolones), cell wall biosynthesis (β-lactams), folate biosynthesis, membrane

integrity (polymyxins), and translation (aminoglycosides) show increased bactericidal activity against *P. aeruginosa* when they were combined with AGXX. To investigate AGXX's potential as a stimulating agent for antibiotic activity, we used AGXX720C, a formulation with lower antimicrobial activity that allowed us to control dosage of AGXX more reliably (**Supplementary FIG S1**). We determined the minimal inhibitory concentrations (MIC) of AGXX720C and ten members of five different antibiotic classes in PA14, which were cultivated under aerobic conditions in Mueller-Hinton broth (**Supplementary Table S1**). Using time killing assays, we exposed PA14 to sublethal concentrations of AGXX720C (75 µg/ml), the indicated antibiotics, and their combinations at the same sublethal concentrations that were used for the individual treatments, respectively. We monitored colony forming units counts every 60 min over a time course of three hours (**Supplementary FIG S2**) and calculated the percent survival for each sample at the 3-hour time point relative to the untreated control (**FIG 2)**. None of the individual treatments with either 75 µg/ml AGXX720C or any of the antibiotics resulted in substantial killing of PA14 (**FIG 2; Supplementary FIG S2**). The combination of 75 µg/ml AGXX720C with 35 ng/ml ciprofloxacin and 100 ng/ml norfloxacin, respectively, resulted in PA14 survival comparable to the individual treatments suggesting that AGXX does not potentiate the bactericidal activities of fluoroquinolones against PA14 (**FIG 2A; Supplementary FIG S2A, B**). Likewise, the combined treatments of AGXX720C and 78 µg/ml carbenicillin, 0.156 µg/ml imipenem, or 125 µg/ml trimethoprim did not significantly change PA14 survival compared to their individual treatments (**FIG 2B, C; Supplementary FIG S2C**). On the other hand, we found that the bactericidal activity of the membrane targeting antibiotic polymyxin B was increased by the presence of AGXX720C as evidenced by a 1-log reduction in PA14 survival as compared to AGXX or polymyxin B alone, which each caused less than 5% killing (**FIG 2D; Supplementary FIG S2D**). However, we observed the most drastic decrease in PA14 survival when AGXX720C was combined with a member of aminoglycoside antibiotics, even at concentrations far below the MIC. Co-treatment of AGXX720C with 0.4 µg/ml gentamicin (Gm) (0.2x MIC) reduced PA14 survival by as much as 4 logs after three hours of treatment (**FIG 2E; Supplementary FIG S2E**), while combinations of AGXX720C with 2 µg/ml amikacin (0.27x MIC), 1 µg/ml tobramycin (0.4x MIC), or 3 µg/ml streptomycin

(0.15x MIC) caused up to 3 log reduction in survival (**FIG 2E, Fig Supplementary S2F-H**).

AGXX increases the sensitivity of *P. aeruginosa* strain PA14 to kanamycin. Considering the significant increase in lethality upon concurrent exposure of PA14 to AGXX720C and aminoglycosides, we sought to determine whether the addition of AGXX720C could reintroduce sensitivity in aminoglycoside-resistant *P. aeruginosa* strains. Like many other *P. aeruginosa* strains, PA14 is intrinsically resistant to many different antibiotics, including the aminoglycoside kanamycin. Under the conditions tested, our PA14 strain showed a MIC of 240 µg/ml for kanamycin. We then exposed PA14 to 75 µg/ml AGXX720C, 50 µg/ml kanamycin, or a combination of 75 µg/ml AGXX720C and 50 µg/ml kanamycin and determined their survival over the time course of 3 hours as described before. As early as 60 minutes post treatment, the combination of AGXX720C and kanamycin reduced colony survival by ~1.5 log, which increased to about 4 log (10,000-fold) difference in survival after 3 hours (**FIG 3**). In summary, we conclude from our data that AGXX potentiates the activity of a wide range of aminoglycoside antibiotics, potentially making aminoglycoside-resistant *P. aeruginosa* strains more sensitive again.

The combination of sublethal concentrations of AGXX and aminoglycosides increases ROS formation and causes DNA damage and protein aggregation. AGXX's main antimicrobial mode of action is mediated by the generation of ROS (12, 16)**.** Increased endogenous oxidative stress has also been linked to the lethality of aminoglycosides and other bactericidal antibiotics (27, 28). It may therefore be possible that a disruption in the redox balance during antibiotic exposure increases lethality by amplifying the adventitious generation of ROS by antibiotics. Thus, we quantified intracellular ROS levels using the redox-sensitive molecular probe dichlorodihydrofluorescein diacetate (H_2DCFDA). H_2DCFDA has been extensively demonstrated to detect various ROS, including peroxides as well as peroxyl- and hydroxyl radicals (29). We treated exponentially growing PA14 for 60 min with sublethal concentrations of Gm (0.25 µg/ml), AGXX720C (50 µg/ml), or their combination and compared H2DCFDA fluorescence in each sample to the untreated control. Individual

treatments with either Gm or AGXX720C did not result in a significant increase in H_2DCFDA fluorescence, excluding the possibility that substantial amounts of ROS were formed at these sublethal concentrations (**FIG 4A**). However, when applied in combination, we observed an 8-fold increase in H_2DCFDA fluorescence indicative of increased ROS production under these conditions. Pre-treatment of PA14 with the ROS scavenger thiourea (30) or the hydrogen peroxide-detoxifying enzyme catalase resulted in a significant decline in H_2DCFDA fluorescence (**FIG 4A**) as well as restored PA14 survival by 2- to 4-log (**FIG 4B; Supplementary FIG S3A**). Thus, our data suggest that the high antimicrobial activity of the combinational treatment can at least in parts be explained by increased ROS formation. However, H_2DCFDA is rather unspecific and detects numerous ROS compounds. We therefore followed up on our observation with the use of additional, more specific ROS-detecting fluorescent dyes. We used the boronate-based peroxy orange 1 (PO1) dye as well as hydroxyphenyl fluorescein (HPF) to examine intracellular concentrations of hydrogen peroxide and hydroxyl radical levels, respectively. After 1 hour of treatment, we detected a significant shift in PO1 and HPF fluorescence, indicating that both hydrogen peroxide and hydroxyl radicals are produced in AGXX720C/Gm-treated PA14 (**FIG 4C, D; Supplementary FIG S3B, C**).

Microorganisms have evolved intricate systems to maintain and restore a balanced redox homeostasis and repair ROS-mediated damage [recently reviewed in (5, 31–35)]. Proteins and nucleic acids represent two of the most susceptible targets of ROS (36, 37). To test whether the elevated ROS production causes macromolecular damage in PA14 cells treated with Gm and AGXX alone and in combination, we analyzed the transcript level of *ipbA* and *sulA,* two genes that have previously been shown to be upregulated in the presence of oxidants such as hypochlorous acid. *ibpA* encodes a molecular chaperone, which plays a significant role in protecting bacteria from proteotoxic stressors (40). *sulA* encodes the cell division inhibitor SulA, which is part of the SOS response and induced when the cell experiences DNA damage (41). We exposed exponentially growing PA14 cells to sublethal concentrations of AGXX720C, Gm, or the combination thereof for 60 min and quantified *ibpA/sulA* mRNA level. While individual treatments with sublethal concentrations of AGXX720C or Gm did not cause significant changes in *ibpA/sulA* expression, their transcript levels were approximately 5-fold (*sulA*) and 100-fold (*ibpA*)

increased when PA14 was treated with the combination of AGXX720C and gentamicin, indicating significant macromolecule damage **(FIG 4E)**.

Antioxidant systems provide protection against ROS-mediated damage caused by a combinational treatment of AGXX and aminoglycosides. To further investigate the role of ROS for the synergistic activity between aminoglycosides and AGXX, we tested the susceptibility of PA14 strains with transposon insertions in genes that have previously been identified as major oxidative stress response and/or defense systems. We exposed PA14 transposon mutant strains with defects in *oxyR* (encodes ROS-sensing transcriptional regulator OxyR), *katA* (encodes catalase KatA), *katB* (encodes catalase KatB), and *dps* (encodes an iron acquisition protein in response to oxidative stress) to the combination of AGXX720C (25 µg/ml) and tobramycin (0.25 µg/ml) for 3 hours and compared their colony survival to that of the corresponding wildtype strain PA14 (**FIG 5**). We found that strains deficient in functional copies of *katA* and *dps* showed a little over 1 log reduced survival compared to wildtype cells, while no difference in survival was observed for cells lacking the hydrogen peroxide global regulator OxyR and catalase KatB, respectively (**FIG 5**). Taken together, our findings point towards a relevant role that ROS generation plays for the synergistic interaction between aminoglycosides and AGXX.

The synergy between AGXX and aminoglycosides on PA14 killing is in parts mediated by a disruption in iron homeostasis. Fe/S cluster are essential cofactors in various metabolic enzymes, including members of the electron transport chain and the TCA cycle (42). Fe/S cluster are particularly vulnerable to ROS, which negatively impacts the activity of metabolic enzymes and ultimately affects cellular metabolism during periods of oxidative stress. Likewise, silver has been found to disrupt Fe/S clusters in proteins (10), resulting in a cellular increase in free iron, which in turn can stimulate hydroxyl radical formation via Fenton reaction and cause extensive macromolecular damage (7). Given the elevated hydroxyl radical level (**FIG 4D; Supplementary FIG S3C**) and increased susceptibility of a *dps*-deficient strain upon PA14 exposure to the AGXX/Gm combination (**FIG 5**), we wondered whether the increased ROS production impairs the activity of Fe/S cluster-containing enzymes. We prepared cell lysates of the

four samples that were prepared as described before and measured the activity of aconitase, an Fe/S-containing enzyme of the TCA cycle, whose activity depends on the presence of the Fe/S-cluster. While individual treatments with sublethal AGXX720C or Gm concentrations had no impact on aconitase activity, exposure to a combination of AGXX720C and Gm resulted in ~75% loss in activity (**FIG 6A**). The loss in aconitase activity could be explained by the release of iron atoms, as it occurs during Fe/S cluster oxidation under superoxide and hydrogen peroxide stress (42, 43). To test the role of free iron for the synergistic effect between AGXX720C and aminoglycosides, we treated PA14 with the iron chelator 2',2' bipyridyl prior to their exposure to sublethal concentrations of AGXX720C and Gm. Indeed, we found that PA14 survival was less impaired when cells had been treated with 2',2' bipyridyl prior to the presence of the AGXX720C/Gm cocktail **(FIG 6B).** Overall, our data suggest an important role of free iron for the ROS-mediated toxicity of aminoglycoside exposure when in synergy with AGXX.

Combined AGXX and aminoglycoside treatment induces significant membrane damage. Considering the exponential and rapid increase in killing when aminoglycosides were administered in combination with AGXX, we were interested in the underlying reasons for this synergistic relationship. In the initial stages of aminoglycoside uptake, the polycationic aminoglycoside electrostatically interacts with the bacterial outer membrane, displacing membrane divalent cations and inevitably increasing membrane permeability (44). Thus, several compounds with membrane permeabilizing properties have been reported as potent aminoglycoside adjuvants (45, 46). To probe the role of membrane permeability, we evaluated outer membrane disruption using the hydrophobic fluorescent probe N-phenyl-1-napthylamine (NPN), which has diminished fluorescence in the presence of an intact outer membrane. NPN fluorescence significantly increases when the dye is bound to exposed phospholipid groups in a disrupted lipopolysaccharide monolayer (47). We found that in contrast to individual treatments with sublethal AGXX720C and Gm concentrations, a combined treatment significantly increased NPN uptake, resulting in ~7-fold higher NPN fluorescence (**FIG 7A**). Next, we examined the inner membrane permeability of PA14 cells that were subjected to AGXX720C and Gm treatment alone and in combination, using the fluorescent probe propidium iodide (PI). Due to its size and charge, PI can only cross compromised inner membranes where it

binds nonspecifically to nucleic acids enhancing its fluorescence exponentially (48). Individual treatments with sublethal AGXX720C and gentamicin concentrations did not result in significantly increased PI fluorescence (**FIG 7B**) suggesting that at these concentrations none of the individual stressors causes significant plasma membrane damage. A combined treatment, however, led to substantially increased PI fluorescence. Our spectrophotometric findings were complemented by fluorescent microscopy analyses of PA14 cells that were treated as described before, washed in PBS, stained with Syto9/PI (live/dead stain), incubated in the dark for 15 minutes at room temperature, mounted onto a glass slide with 1% agarose, and imaged at 60x magnification via inverted confocal microscopy. While the individual treatments with 0.25 µg/ml Gm or 50 µg/ml AGXX720C only caused increased PI fluorescence in very few cells, the number of PI-stained cells was substantially higher in PA14 cells that were treated with a combination of sublethal AGXX720C/Gm concentrations (**FIG 7C**).

AGXX increases aminoglycoside uptake and lethality through increased activity of the proton motive force (PMF). Considering the significance of membrane permeability for aminoglycoside uptake, we reasoned that the increased membrane disruption PA14 experiences during a combined treatment of AGXX and aminoglycosides would facilitate intracellular accumulation of aminoglycosides. Using flow cytometry, we evaluated the uptake of Texas-Red-labeled Gentamicin (TR-Gm) in exponentially growing PA14 in the presence or absence of AGXX720C. Treatment of PA14 with a combination of AGXX720C and TR-GM resulted in a significant increase in TR-Gm uptake similar to treatment with the membrane-targeting antibiotic polymyxin B (**FIG 8A, Supplementary FIG S4A).** The increased uptake of TR-Gm in the presence of AGXX resulted in a 2.5 log reduction in bacterial survival compared to PA14 that were only exposed to TR-Gm alone **(Supplementary FIG S4B**). Moreover, the secondary and tertiary stage of aminoglycoside import appears to depend on an active membrane potential and occurs therefore only in actively respiring cells (44, 49). As such, increasing cellular respiration or stimulation of membrane potential has been found to increase aminoglycoside lethality. Using the protonophore CCCP, a compound that efficiently inhibits the proton motive force (PMF), we determined whether the synergy between AGXX and aminoglycosides is dependent on the membrane potential. Not surprisingly, PA14 killing by a lethal dose

of gentamycin (1 µg/ml) could be reduced by almost 2 logs when the cells were pre-incubated with CCCP (**Supplementary FIG S4C).** Likewise, pretreatment with CCCP restored PA14 survival to a similar degree in the presence of 0.25 µg/ml Gm and 50 µg/ml AGXX720C for three hours **(Fig. 8B).** Surprisingly, combining polymyxin B at 1x MIC and 2x MIC with sublethal gentamicin concentrations did not result in increased killing relative to polymyxin B alone **(Fig. S2D)**. Overall, our findings indicate that AGXX's synergistic effect on aminoglycoside lethality does not only involve increased membrane permeability but also requires an active proton motive force across the bacterial membrane.

Discussion

In the present study, we provide evidence for a potential suitability of the novel silver containing antimicrobial AGXX as an antibiotic adjuvant with activity on the opportunistic pathogen *P. aeruginosa*. We show that AGXX serves as an efficient tool to potentiate the activity of aminoglycoside antibiotics by reducing bacterial survival up to 50,000-fold. Aside from a 1-log increase in killing found when the ROS-producing Ag/Ru complex was combined with the membrane-targeting antibiotic polymyxin B, AGXX did not influence the activity of antibiotics targeting DNA replication, cell wall synthesis, or folate metabolism **(FIG 2)** raising the possibility that AGXX's potentiating effects could be linked to a malfunction in protein synthesis. AGXX's potentiating effect was not limited to select aminoglycosides but applied to all members tested including gentamicin, streptomycin, amikacin, and tobramycin (**FIG 2**). Additional support for AGXX's stimulating effect on aminoglycoside activity was provided by its ability to re-sensitize a kanamycin resistant *P. aeruginosa* strain (**FIG 3**). Notably, both AGXX and aminoglycoside antibiotics were present at concentrations far below their MICs (0.1-0.3x MIC) indicating that the combination between the compounds was quite powerful with regards to increasing the bactericidal activity of aminoglycosides.

Based on our findings, we propose the following model for the synergy between AGXX and aminoglycoside antibiotics (**FIG 9**): The antimicrobial action of AGXX is mediated by superoxide (O_2^-) and hydrogen peroxide (H_2O_2), which are generated in a redox cycle

between silver (Ag) and ruthenium (Ru^{x+1}) (15, 16). While the location of AGXX-mediated ROS production was not the focus of his study, we propose that ROS is mainly generated in the extracellular part before the compounds penetrate the cell. This assumption is based on our finding that exogenous addition of catalase was highly effective in reducing ROS level and increasing *P. aeruginosa* survival upon treatment with a combination of AGXX and Gm (**Supplementary FIG S3A**), given that catalase cannot readily cross the bacterial cell envelope. The combination of AGXX and aminoglycosides concertedly increased endogenous ROS levels, including hydrogen peroxide and hydroxyl radicals. Potentially intensified by released silver ions, the increased ROS level may disrupt iron-sulfur clusters in metabolic enzymes such as aconitase, resulting in the release of free iron, which ultimately triggers hydroxyl radical (OH•) formation in a Fenton reaction. Increasing ROS levels can inflict macromolecule damage such as in DNA, proteins, and lipids, as evidenced by *(i)* the increased expression of members of the SOS and heat shock responses, and *(ii)* the possibility that the observed damage on outer and inner membrane is mediated by ROS. In either way, increased ROS production contributes to the enhanced killing of *P. aeruginosa* upon treatment with a combination of AGXX and aminoglycosides. The synergistic effect between AGXX and aminoglycosides is also mediated by an increased uptake and the cellular accumulation of aminoglycosides, which can be attenuated by disrupting the bacterial membrane potential with ionophores such as CCCP.

The antimicrobial effects of silver and silver containing agents have been extensively documented (50–52). However, in spite of the increasing use of silver in antimicrobial applications, its mechanism of action remains to be poorly understood (24, 53, 54). Silver along with other ROS inducing agents have been proposed to induce an array of multimodal cytotoxic events, including the mis-metalation of proteins, DNA damage, and imbalanced redox homeostasis, which ultimately disrupt multiple bacterial networks leading to cell death (5, 17, 55). Thus, we investigated whether AGXX, through its multimodal effects as an ROS inducing compound, could increase that activity of conventional antibiotics against *P. aeruginosa*. AGXX itself has been proposed to exert its antimicrobial action through the generation of ROS rather than the release of silver ions. AGXX-mediated ROS production likely starts with the generation of superoxide,

which subsequently can be dismutated by cellular superoxide dismutases into hydrogen peroxide (15, 56). Likewise, aminoglycosides have also been posited to induce metabolic alterations that induce endogenous ROS level (57). We found a significant increase in hydrogen peroxide and hydroxyl radical signals upon exposure of PA14 to a combination of AGXX and aminoglycoside as evidenced by increased PO1 and HPF fluorescence **(FIG 4)** and decreased survival of transposon insertion strains defective in KatA and Dps **(FIG 5)**. Surprisingly, a transposon insertion into the *oxyR* gene, encoding the major hydrogen response regulator OxyR, did not show a significant difference in survival relative to the wildtype under combined AGXX/aminoglycoside exposure **(FIG 5)**. However, this is consistent with a previous study on the aminoglycoside potentiating effects of silver nitrate, in which neither *oxyR*-deficient strains nor strains that constitutively express OxyR had significant effects on bacterial survival (58). On the other hand, the overexpression of the H_2O_2 detoxifying gene *ahpF* attenuated the lethality and proteotoxic effects of aminoglycosides, providing evidence for the relevance of hydrogen peroxide in aminoglycoside toxicity (59). Previous studies have demonstrated that pretreatment with antioxidant molecules such as thiourea reduced intracellular hydroxyl radical levels and increased bacterial survival during aminoglycoside and silver stress (17, 28, 60, 61). Consistent with these findings, we made similar observations as the addition of either catalase or thiourea to AGXX-aminoglycoside-treated PA14 resulted in a significant reduction in endogenous ROS level as well as bacterial killing relative to the combined treatment alone **(FIG 4A, B; Supplementary FIG S3A)**. Given that individual AGXX or gentamicin treatments did not result in a significant increase in ROS signals, it is plausible that applying these antimicrobials at concentrations far below the MIC would not induce the physiological/metabolic alterations necessary for aggravating endogenous ROS levels.

Considering that both superoxide and silver ions have been reported to destabilize Fe/S cluster proteins resulting in the release of solvent-exposed iron (10, 62), we investigated the effects of individual and combinational treatments with AGXX and/or aminoglycoside antibiotics on the activity of aconitase, an Fe-S cluster containing enzyme. We found aconitase to be extremely sensitive towards exposure to both antimicrobials when administered in combination (**FIG 6A**). Disrupted Fe-S clusters could potentially lead to

an increase in intracellular iron levels and subsequent OH• generation through Fenton reaction as it has been demonstrated under hydrogen peroxide stress in ROS-sensitive *E. coli* strains (63). This would explain the significantly higher OH• levels detected in PA14 cells that were exposed to a combined AGXX and gentamicin mixture **(FIG 4)**, which could cause significant DNA damage and induce the SOS response. In fact, we found that the combination of sublethal AGXX and gentamicin significantly induced the expression of *sulA,* an SOS response marker of DNA damage **(FIG 4E)**. Likewise, addition of 2',2' bipyridyl resulted in a 1-log increase in bacterial survival when cells were exposed to the toxic cocktail of gentamycin and AAGXX suggesting that free iron contributes to the bactericidal effects **(FIG 6B)**. All in all, our findings highlight the relevance of oxidative stress in the enhancement of antibiotic lethality in *P. aeruginosa* exposed to sub-inhibitory concentrations of AGXX and aminoglycosides.

Compared to other gram-negative pathogens, *P. aeruginosa* possesses high intrinsic resistance mechanisms towards a variety of antibiotics (64). This resistance is mediated in part by its extensive arsenal of efflux pumps and significantly lower outer membrane permeability (64). We found that combining AGXX and gentamicin increased both inner and outer membrane permeability in *P. aeruginosa* leading to a subsequent increase in aminoglycoside uptake **(FIG 7, FIG 8)**. Aminoglycosides are polycationic in nature and known to displace divalent cations that cross-bridge lipopolysaccharides, which makes the outer membrane substantially more permeable (65, 66). It is therefore possible that AGXX, much like aminoglycosides, disrupts the outer leaflet of the outer membrane, with the result that lower amounts of aminoglycosides are required to permeabilize *P. aeruginosa*. If this was true, we would suspect that the initial stages of aminoglycoside uptake could likely be accelerated causing a more rapid antibiotic influx. Surprisingly, we found that the addition of sublethal polymyxin B concentrations did not affect gentamicin lethality indicating that the mechanism behind the potentiating effects of AGXX extends beyond increased membrane permeability **(FIG S4D)**. We further found that disrupting membrane potential using an ionophore increased bacterial survival under combined AGXX and gentamicin stress **(FIG 8)**, suggesting an important role for the energy dependent phase of aminoglycoside uptake AGXX's potentiating effect. By definition, antibiotic adjuvants do not possess inherent antimicrobial activity (67). Even though

AGXX can technically not be defined as an antibiotic adjuvant given its own antimicrobial activity (16), our use of sublethal AGXX concentrations to screen for potentiating effects satisfied this definition. Notably, the antimicrobial properties of silver have been accepted for a long time and taken advantage of in topical ointments such as silverdene cremes to prevent and treat *P. aeruginosa* infections in burn wound patients (26). A comparison to silver nitrate and silver sulfadiazine (silverdene) revealed an increased potency of some of the AGXX formulations resulting in a lower survival rate of PA14 **(FIG 1)**. Moreover, given that antibacterial combination therapies typically involve significantly lower concentrations of the antimicrobials compared to what is needed for individual treatments, such approaches would potentially delay resistance development.

Materials and Methods

Bacterial strains and growth conditions. Unless stated otherwise, overnight *P. aeruginosa* PA14 strains **(Supplementary Table 2)** were grown under aerobic conditions in Luria-Bertani broth (LB, Millipore Sigma) at 37°C for 16-20 hours at 300 rpm. For subsequent assays, overnight cultures were diluted into Mueller-Hinton broth or 3-(N-morpholino) propanesulfonic acid minimal media containing 0.2% glucose, 1.32 mM K_2HPO_4 and 10 µM thiamine (MOPSg) and incubated at 37 °C at 300 rpm.

Minimum Inhibitory Concentration (MIC). MIC assays were performed in 96-well plates in a total volume of 200 µl per well. Overnight PA14 cultures were diluted into Mueller-Hinton broth to an OD_{600} of 0.002 and distributed into 96 well plates that contained increasing concentrations of ciprofloxacin, nalidixic acid, carbenicillin, imipenem, trimethoprim, polymyxin B, gentamicin, amikacin, tobramycin, streptomycin, and kanamycin, respectively. Plates were subsequently incubated at 37 °C for 16 hours at 300 rpm. MIC assays were performed in duplicates. The MIC is defined as the lowest antibiotic concentration that inhibited growth.

Time Killing Assays. Overnight PA14 cultures were diluted ~25-fold into Mueller-Hinton broth by normalizing cultures to an OD_{600} = 0.1 in a 6-well sterile cell culture plate. Sublethal concentrations of AGXX720C and antibiotics of interest were added individually

and in combination as indicated and plates incubated at 37°C for 3 hours at 150 rpm under aerobic conditions. CCCP and BIP were added 60 minutes prior to AGXX/aminoglycoside treatments whenever indicated. At 1-hour intervals, OD_{600} of cultures were recorded, sample volumes were normalized to the lowest optical density measured, serially diluted in PBS (pH = 7.4) and plated on LB agar to quantify colony forming units (CFU) after 16 hours. Percent survival was calculated as the ratio of surviving colonies from treated to untreated samples.

Intracellular ROS level. Intracellular ROS levels were quantified using the redox-sensitive dye 2',7'-dichlorodihydrofluorescein diacetate (H_2DCFDA) (Thermofisher Scientific). Exponentially growing PA14 cultures were left untreated or treated with 0.25 µg/ml Gm, 50 µg/ml AGXX720C or a combination of both for 1 hour. Samples were collected and normalized to an OD_{600}=1.0. Cells were washed twice, resuspended in prewarmed PBS containing 10 µM H_2DCFDA, and incubated in the dark at 37 °C for 30 min before samples were washed twice again in PBS and DCF fluorescence measured at excitation/emission wavelengths of 485/535 nm (Tecan 200 plate reader). To quench cellular ROS, cells were pretreated with 50 mM thiourea prior to the stress treatments.

Quantification of hydrogen peroxide level. The monoborate fluorescent probe peroxy orange 1 (PO1) was used to measure hydrogen peroxide level. Exponentially growing PA14 cultures were treated with 10 µM PO1 prior to their exposure to 0.25 µg/ml Gm, 50 µg/ml AGXX720C, or a combination of both for 1 hour. Cells were washed twice and resuspended in prewarmed PBS. Samples were analyzed using the flow cytometer (BD FACS melody) in the FITC channel (613/18 filter). At least 10,000 events were recorded, and figures generated using FCSlayzer.

Quantification of Hydroxyl radical level. The fluorescent probe hydroxyphenyl fluorescein (HPF; Invitrogen) was used to determine the amount of cellular hydroxyl radicals produced (68). Exponentially growing PA14 cultures were either left untreated or treated for 1 hour with 0.25 µg/ml Gm, 50 µg/ml AGXX720C, or the combination thereof. Samples were collected and normalized to an OD_{600nm} of 1.0 after washing twice with PBS (pH 7.4). Cells were then stained with 10 µM HPF and incubated in the dark for 30 minutes at 37 °C. Cells were washed twice and resuspended in prewarmed PBS.

Samples were analyzed using the flow cytometer (BD FACS melody) in the FITC channel (527/32 filter). At least 10,000 events were recorded, and figures generated using FCSlayzer.

Gene expression analyses by qRT-PCR. Overnight PA14 cultures were diluted into MOPSg media to an OD_{600}=0.1 and grown to mid-log phase (OD_{600nm}=0.3). Cultures were left untreated or treated with 0.25 µg/ml Gm, 50 µg/ml AGXX720C, or the combination thereof for 60 minutes. Transcription was stopped by the addition of an equal volume of ice-cold methanol. Total RNA was extracted from three biological replicates using a commercially available RNA extraction kit (Macherey & Nagel). Remaining DNA was removed using the TURBO DNA-free kit (Thermo Scientific). mRNA was reverse transcribed into cDNA using the PrimeScript cDNA synthesis kit (TaKaRa). qRT-PCRs were set up according to the manufacturer's instructions (Alkali Scientific). Transcript levels of the indicated genes were normalized against transcript levels of the 16S rRNA-encoding *rrsD* gene and relative fold changes in gene expression were calculated using the $2^{-\Delta\Delta CT}$ method (69). The following primer pairs were used for gene amplification: *ipbA*, TTCCGTCATTCCGTAGG & AGGTCTTCTTCCTGG; *sulA,* ACTGTTCCAGGAAGCGTTCT & AGCGAAAGTTCGCTAAAGGC; *rrsD,* TATCAGATGAGCCTAGGTCGGATTA & TTTACAATCCGAAGACCTTCTTCAC.

Aconitase Assay. Exponentially growing PA14 were treated with sublethal concentrations of AGXX720C (100 µg/ml), Gm (0.6 µg/ml) or the combination thereof. Aconitase activity was measured from cell lysates using the Aconitase Assay Kit (Abcam) according to manufacturer's instructions. One unit of aconitase is defined as the amount of enzyme that isomerizes 1 µmol of citrate to isocitrate per min at pH 7.4 and 25 °C.

Outer membrane permeability assay. The N-phenyl-1-naphthylamine (NPN) uptake assay was used to detect outer membrane damage as described in (70). Exponential phase PA14 were treated with 0.25 µg/ml Gm, 50 µg/ml AGXX720C, a combination thereof. Addition of 2 µg/ml polymyxin B was used as a positive control. Cells were collected after 60 min of treatment, washed, and resuspended to an OD_{600}=0.5 in HEPES-sodium buffer (pH 7.2). 10 µM NPN was added, and samples incubated in the dark for 15

min. NPN fluorescence was measured at excitation/emission wavelengths of 350/420 nm. Increased NPN uptake (indicating outer membrane damage) was calculated using the following equation (71):

$$NPN\ uptake = \frac{Sample_{+NPN} - Sample_{-NPN}}{Hepes\ Buffer_{+NPN} - Hepes\ Buffer_{-NPN}}$$

Inner membrane disruption assay. Inner membrane integrity was determined by the cellular uptake of propidium iodide following antimicrobial treatments. Exponentially growing PA14 cells were either left untreated or treated with 0.25 µg/ml Gm, 50 µg/ml AGXX720C, or a combination thereof. Cells were harvested after 1 hour, washed twice, and resuspended in PBS (pH 7.4) at an OD_{600}=0.5. Propidium iodide (Thermo Fisher Scientific) was added to a final concentration of 500 nM and samples incubated in the dark for 30 min. Fluorescence intensities were measured at excitation/emission wavelengths of 535/617 nm. Samples treated with polymyxin B at a sublethal concentration (2 µg/ml) were included as a positive control.

LIVE/DEAD staining. Exponentially growing PA14 cells were either left untreated or treated with 0.25 µg/ml Gm, 50 µg/ml AGXX720C, or a combination thereof. Cells were harvested after 1 hour, washed twice, and resuspended in PBS (pH 7.4) at an OD_{600}=0.2. Samples were stained with SYTO9 (6µM) and PI (30 µM) and incubated in the dark for 15 min at room temperature**.** Cells were then transferred onto a glass slide and covered with 1% agarose prior to visualization using a Leica SP2 confocal microscope. Samples treated with polymyxin B at a sublethal concentration (2 µg/ml) were included as a positive control.

Texas Red-Gentamicin Uptake Assay. Texas Red-succinimidyl ester (Invitrogen) was dissolved to a final concentration of 20 mg/ml in high quality anhydrous N,N-dimethylformamide at 4 °C (72). Gm was dissolved in 100 mM K_2CO_3 (pH 8.5) to a final concentration of 10 mg/ml at 4 °C. 20 ul Texas Red was slowly added dropwise to 700 ul Gm to allow for the conjugation reaction to obtain the Texas-Red labeled gentamicin (TR-Gm) (72). The TR-Gm conjugate was diluted in water and stored at -20 °C protected from light. Exponentially growing PA14 cells were first treated with 1 µg/ml TR-Gm followed by exposure to either 50 µg/ml AGXX720C or 2 µg/ml polymyxin B (positive control). After 1

hour incubation in the dark at 37 °C, cells were collected and analyzed in the flow cytometer (BD FACS melody) using the 697/58 filter. At least 10,000 events were recorded, and figures generated using FCSlayzer.

Statistical analyses: All statistical analyses were performed in GraphPad prism version 8.0.

ACKNOWLEDGEMENTS

This work was supported by the NIAID grant R15AI164585 and the Illinois State University Pre-Tenure Faculty Initiative Grant (to J.-U. D.). G.Y.D. was supported by Weigel and Mockford-Thompson grants by the Phi-Sigma Biological Sciences Honors Society. G.M.A. and C.D.O. were supported by the Illinois State University Undergraduate Research Support Program. Dr. Uwe Landau and his team from Largentec GmbH are acknowledged for scientific discussion and providing the AGXX formulations. We also thank Sadia Sultana for critically proof-reading the manuscript and providing invaluable feedback. Figure 9 was generated with Adobe Illustrator.

FIGURE LEGENDS

FIG 1 AGXX394 is more efficient in killing *P. aeruginosa* than silverdene and silver nitrate. Overnight PA14 cultures were diluted ~25-fold into MOPSg media (OD_{600}=0.1) and treated for three hours with 25 µg/ml $AgNO_3$ (black symbol), silverdene (grey symbol), and AGXX394 (red symbol), respectively. Colony survival was evaluated every hour by serially diluting samples and plating them onto LB agar. Percent survival was calculated relative to the untreated control (*n=4, ± S.D).*

FIG 2 AGXX exponentially increases the activity of aminoglycosides against *P. aeruginosa*. Overnight PA14 cultures were diluted ~25-fold (OD_{600}=0.1) into Mueller-Hinton media and exposed to 75 µg/ml AGXX720 (black bars), a sublethal concentration of the indicated antibiotic (grey bar), or the combined treatment of both (red bars) for 3 hours. Samples were taking every 60 min, serial diluted, plated on LB agar, and incubated

for 20 hours for CFU counts. Percent survival was calculated relative to the untreated control for: **(A)** 35 ng/ml ciprofloxacin and 100 ng/ml nalidixic acid, respectively; **(B)** 78 µg/ml carbenicillin and 0.156 µg/ml imipenem, respectively; **(C)** 125 µg/ml trimethoprim; **(D)** 1.5 µg/ml polymyxin B; and **(E)** 0.4 µg/ml gentamicin, 2.0 µg/ml amikacin, 1.0 µg/ml tobramycin, and 3 µg/ml streptomycin, respectively. All experiments were performed in at least three biological replicates and error bars represent mean ± SD. * $p < 0.05$, ** $p < 0.01$, *** $p < 0.001$ (Student's t test, calculated relative to cultures treated with antibiotics alone).

FIG 3 AGXX increases the sensitivity of *P. aeruginosa* strain PA14 to kanamycin. Overnight PA14 cultures were diluted ~25-fold into Mueller-Hinton media (OD_{600}=0.1) and either left untreated or exposed to 75 µg/ml AGXX720C, 50 µg/ml kanamycin, or the combination thereof for 3 hours. Samples were taken every 30 minutes, serial diluted and plated on LB agar for CFU counts, (*n=4, ± S.D)*.

FIG 4 The combination of sublethal concentrations of AGXX and aminoglycosides increases ROS formation and causes DNA damage and protein aggregation. Mid-log PA14 cells were treated with sublethal concentrations of Gm (0.25 µg/ml), AGXX720C (50 µg/ml), the combination thereof, or left untreated. **(A)** Intracellular ROS levels were quantified by H_2DCFDA fluorescence. 50mM thiourea was used as a ROS quencher (*n=3, ± S.D)*. **(B)** Samples were serially diluted in PBS after 60 min of incubation, spot-titered onto LB agar and incubated for 20 hours. One representative of three independent experiments with similar outcomes. **(C, D)** Cells were strained with **(C)** 10 µM peroxy-orange 1 (PO1) and **(D)** 10µM hydroxyphenyl fluorescein (HPF) for 60 min and fluorescence was measured via flow cytometry (*n=3, ± S.D)*. **(E)** The induction of *sulA* (white bar) and *ibpA* (black bar) transcript levels was determined by qRT-PCR. Gene expression was normalized to the housekeeping gene *rrsD* and calculated as fold changes based on expression levels in the untreated control (*n=3, ± S.D.*). One-way ANOVA, Dunnett's posttest; *ns=p>0.05,* * $p < 0.05$, ** $p < 0.01$, *** $p < 0.001$, **** $p < 0.0001$.

FIG 5 Antioxidant systems provide protection against ROS-mediated damage caused by a combinational treatment of AGXX and aminoglycosides. Overnight

cultures of PA14 wildtype, Δ*oxyR,* Δ*katA,* Δ*katB* and Δ*dps* were diluted into MOPSg to an OD_{600}=0.01 and grown under aerobic conditions until OD_{600}=0.1. Cultures were either left untreated (grey bars) or treated with a combination of 0.25 µg/ml tobramycin and 25 µg/ml AGXX720C (white bars). Bacterial survival was quantified after two hours by serially diluting cells in PBS and plating on LB agar for 20 hours at 37°C (*n=3,* ± *S.D*). Student t-test, * $p < 0.05$).

FIG 6 The synergy between AGXX and aminoglycosides on PA14 killing is in parts mediated by a disruption in iron homeostasis. Overnight PA14 cultures were diluted into MOPSg and incubated under aerobic conditions until exponential phase was reached. **(A)** Cells were left untreated or treated with 100 µg/ml AGXX720C, 0.6 µg/ml Gm, or the combination thereof for 1 hour. Aconitase activities were determined in crude extracts (*n=4,* ± *S.D*). One-way ANOVA, Dunnett's posttest; *ns=p>0.05,* ** $p < 0.01$. **(B)** Cultures were either left untreated (white square) or treated with 0.25 µg/ml Gm (white diamond), 50µg/ml AGXX720C (white circle), or the combination thereof (white triangle) for three hours. Survival was determined each hour by serially diluting samples in PBS and plating onto LB agar for overnight growth. The impact of free iron on the increased killing by AGXX/Gm cotreatments was tested by the absence (white triangle) and presence (black diamonds) of 125 µM 2',2' bipyridyl (*n=3,* ± *S.D*.). Student's t test, *=p<0.05).

FIG 7 Combined AGXX and aminoglycoside treatment induces significant membrane damage. PA14 cells grown to mid-log phase in MOPSg media were left untreated or treated with sublethal concentrations of Gm (0.25 µg/ml), AGXX720C (50µg/ml), and the combination thereof. Cells were harvested after 1 hour of treatment, washed in PBS, and stained with **(A)** 10 µM N-phenyl-1-naphthylamine (NPN) dye, and **(B)** 0.5 µM propidium iodide (PI). Fluorescence intensities were determined at excitation/emission wavelengths of **(A)** 350/420 nm and **(B)** 535/617 nm, respectively, (*n=4,* ± *S.D*.). One-way ANOVA, Dunnett's posttest; *ns=p>0.05,* * $p < 0.05$, **** $p <$ 0.0001. **(C)** Samples were washed in PBS, stained with PI/Syto9, incubated in the dark for 15 minutes at room temperature, mounted onto a glass slide with 1% agarose, and

imaged at 60x magnification via inverted confocal microscopy. One representative of three independent experiments with similar outcomes.

FIG 8 AGXX increases aminoglycoside uptake and lethality through increased activity of the proton motive force (PMF). (A) Mid-log PA14 cells were treated with 1.0 µg/ml TR-Gm, 1.0 µg/ml TR-Gm + 50 µg/ml AGXX720C, and 1.0 µg/ml TR-Gm + 2.0 µg/ml polymyxin B (PMB) for 1 hour, respectively. TR-Gm uptake was measured via flow cytometry. **(B)** Mid-log phase PA14 were left untreated (control) or exposed to 0.25 µg/ml Gm, 50 µg/ml AGXX720C or 0.25 µg/ml Gm + 50 µg/ml AGXX720C for 3 hours. Samples were serial diluted, plated on LB agar, and incubated for 20 hours for CFU counts. To test the impact of the PMF on the killing of a combination of AGXX and aminoglycosides, PA14 were pretreated with or without 50 µM carbonyl cyanide *m*-chlorophenyl hydrazone (CCCP) prior to AGXX/Gm exposure *(n=3, ± S.D.)*. Student's t test, ** $p<0.01$.

FIG 9 Proposed model for the synergy between AGXX and aminoglycoside antibiotics. The antimicrobial action of AGXX is mediated by superoxide (O_2^-) and hydrogen peroxide (H_2O_2), which are generated in a redox cycle between silver (Ag) and ruthenium (Ru^{x+1}). The combination of AGXX and aminoglycosides concertedly increases endogenous ROS levels. Potentially facilitated by a release of silver ions, the increased ROS level may disrupt iron-sulfur clusters in metabolic enzymes such as aconitase, resulting in the release of free iron, which ultimately triggers hydroxyl radical (OH•) formation in a Fenton reaction. Increasing ROS levels can inflict macromolecule damage such as DNA damage and protein aggregation, contributing to increased killing as observed for *P. aeruginosa* that were treated with a combination of AGXX and aminoglycosides. The synergistic effect between AGXX and aminoglycosides is also mediated by an increased uptake and the cellular accumulation of aminoglycosides, which can be attenuated by disrupting the bacterial membrane potential with ionophores such as CCCP.

References

1. Llor C, Bjerrum L. 2014. Antimicrobial resistance: risk associated with antibiotic overuse and initiatives to reduce the problem. Therapeutic advances in drug safety 5:229–41.
2. Spellberg B. 2014. The future of antibiotics. Critical Care 18:228.
3. Turner KH, Everett J, Trivedi U, Rumbaugh KP, Whiteley M. 2014. Requirements for Pseudomonas aeruginosa Acute Burn and Chronic Surgical Wound Infection. PLOS Genetics 10:e1004518.
4. Pang Z, Raudonis R, Glick BR, Lin TJ, Cheng Z. 2019. Antibiotic resistance in Pseudomonas aeruginosa: mechanisms and alternative therapeutic strategies. Biotechnology Advances 37:177–192.
5. Chopra I, Hesse L, O'Neill AJ. 2002. Exploiting current understanding of antibiotic action for discovery of new drugs. Symposium series (Society for Applied Microbiology) 31:4S-15S.
6. Shang D, Liu Y, Jiang F, Ji F, Wang H, Han X. 2019. Synergistic Antibacterial Activity of Designed Trp-Containing Antibacterial Peptides in Combination With Antibiotics Against Multidrug-Resistant Staphylococcus epidermidis. Frontiers in Microbiology 0:2719.
7. Barras F, Aussel L, Ezraty B. 2018. Silver and antibiotic, new facts to an old story. Antibiotics 7:1–10.
8. GA S, SE P. 2010. Antibacterial activity of nanosilver ions and particles. Environmental science & technology 44:5649–5654.

9. Liau SY, Read DC, Pugh WJ, Furr JR, Russell AD. 1997. Interaction of silver nitrate with readily identifiable groups: Relationship to the antibacterial action of silver ions. Letters in Applied Microbiology 25:279–283.
10. Xu FF, Imlay JA. 2012. Silver(I), Mercury(II), Cadmium(II), and Zinc(II) Target Exposed Enzymic Iron-Sulfur Clusters when They Toxify Escherichia coli. Applied and Environmental Microbiology 78:3614.
11. Church D, Elsayed S, Reid O, Winston B, Lindsay R. 2006. Burn wound infections. Clinical Microbiology Reviews 19:403–434.
12. Clauss-Lendzian E, Vaishampayan A, de Jong A, Landau U, Meyer C, Kok J, Grohmann E. 2018. Stress response of a clinical Enterococcus faecalis isolate subjected to a novel antimicrobial surface coating. Microbiological Research 207:53–64.
13. Van Loi V, Busche T, Preuß T, Kalinowski J, Bernhardt J, Antelmann H. 2018. The AGXX® antimicrobial coating causes a thiol-specific oxidative stress response and protein s-bacillithiolation in staphylococcus aureus. Frontiers in Microbiology 9:1–15.
14. Sobisch LY, Rogowski KM, Fuchs J, Schmieder W, Vaishampayan A, Oles P, Novikova N, Grohmann E. 2019. Biofilm forming antibiotic resistant gram-positive pathogens isolated from surfaces on the international space station. Frontiers in Microbiology 10:1–16.
15. Linzner N, Antelmann H. 2021. The Antimicrobial Activity of the AGXX® Surface Coating Requires a Small Particle Size to Efficiently Kill Staphylococcus aureus. Frontiers in Microbiology 12.

16. Guridi A, Diederich AK, Aguila-Arcos S, Garcia-Moreno M, Blasi R, Broszat M, Schmieder W, Clauss-Lendzian E, Sakinc-Gueler T, Andrade R, Alkorta I, Meyer C, Landau U, Grohmann E. 2015. New antimicrobial contact catalyst killing antibiotic resistant clinical and waterborne pathogens. Materials Science and Engineering C 50:1–11.
17. Morones-Ramirez J, Winkler JA, Spina CS, Collins JJ. 2013. Silver enhances antibiotic activity against gram-negative bacteria. Science Translational Medicine 5.
18. Kalan L, Wright GD. 2011. Antibiotic adjuvants: multicomponent anti-infective strategies. Expert Reviews in Molecular Medicine 13.
19. Huttner A, Bielicki J, Clements MN, Frimodt-Møller N, Muller AE, Paccaud J-P, Mouton JW. 2020. Oral amoxicillin and amoxicillin–clavulanic acid: properties, indications and usage. Clinical Microbiology and Infection 26:871–879.
20. Brynildsen MP, Winkler JA, Spina CS, MacDonald IC, Collins JJ. 2013. Potentiating antibacterial activity by predictably enhancing endogenous microbial ROS production. Nature biotechnology 31:160.
21. Foti JJ, Devadoss B, Winkler JA, Collins JJ, Walker GC. 2012. Oxidation of the guanine nucleotide pool underlies cell death by bactericidal antibiotics. Science 336:315–319.
22. Soothill G, Hu Y, Coates A. 2013. Can We Prevent Antimicrobial Resistance by Using Antimicrobials Better? Pathogens 2013, Vol 2, Pages 422-435 2:422–435.
23. Feng QL, Wu J, Chen GQ, Cui FZ, Kim TN, Kim JO. 2000. A mechanistic study of the antibacterial effect of silver ions on Escherichia coli and Staphylococcus aureus. Journal of Biomedical Materials Research 52:662–668.

24. Silver S, Phung LT, Silver G. 2006. Silver as biocides in burn and wound dressings and bacterial resistance to silver compounds. Journal of Industrial Microbiology and Biotechnology 33:627–634.

25. Egger S, Lehmann RP, Height MJ, Loessner MJ, Schuppler M. 2009. Antimicrobial Properties of a Novel Silver-Silica Nanocomposite Material. Applied and Environmental Microbiology 75:2973–2976.

26. Fuller FW. 2009. The side effects of silver sulfadiazine. J Burn Care Res 30:464–470.

27. Kohanski MA, Tharakan A, Lane AP, Ramanathan M. 2016. Bactericidal Antibiotics Promote Reactive Oxygen Species Formation and Inflammation in Human Sinonasal Epithelial Cells. International forum of allergy & rhinology 6:191.

28. Kohanski MA, Dwyer DJ, Hayete B, Lawrence CA, Collins JJ. 2007. A Common Mechanism of Cellular Death Induced by Bactericidal Antibiotics. Cell 130:797–810.

29. Kim H, Xue X. 2020. Detection of Total Reactive Oxygen Species in Adherent Cells by 2',7'-Dichlorodihydrofluorescein Diacetate Staining. Journal of visualized experiments : JoVE 2020:1–5.

30. Kelner MJ, Bagnell R, Welch KJ. 1990. Thioureas react with superoxide radicals to yield a sulfhydryl compound. Explanation for protective effect against paraquat. Journal of Biological Chemistry 265:1306–1311.

31. Imlay JA. 2008. Cellular defenses against superoxide and hydrogen peroxide. Annu Rev Biochem 77:755–776.

32. Gray MJ, Wholey W-Y, Jakob U. 2013. Bacterial Responses to Reactive Chlorine Species. Annual Review of Microbiology 67:141–160.

801 33. Varatnitskaya M, Degrossoli A, Leichert LI. 2021. Redox regulation in host-pathogen
802 interactions: thiol switches and beyond. Biological Chemistry 402:299–316.
803 34. Sultana S, Foti A, Dahl J-U. 2020. Bacterial Defense Systems against the
804 Neutrophilic Oxidant Hypochlorous Acid. Infection and Immunity 88:e00964-19.
805 35. Dahl J-U, Gray MJ, Jakob U. 2015. Protein Quality Control Under Oxidative Stress
806 Conditions. J Mol Biol 427:1549–1563.
807 36. Ezraty B, Gennaris A, Barras F, Collet JF. 2017. Oxidative stress, protein damage
808 and repair in bacteria. Nature Reviews Microbiology 2017 15:7 15:385–396.
809 37. Cooke MS, Evans MD, Dizdaroglu M, Lunec J. 2003. Oxidative DNA damage:
810 mechanisms, mutation, and disease. The FASEB Journal 17:1195–1214.
811 38. Groitl B, Dahl J-U, Schroeder JW, Jakob U. 2017. Pseudomonas aeruginosa
812 defense systems against microbicidal oxidants. Molecular Microbiology 106:335–
813 350.
814 39. Sultana S, Crompton ME, Meurer K, Jankiewicz O, Morales GH, Johnson C, Horbach
815 E, Hoffmann KP, Kr P, Shah R, Anderson GM, Mortimer NT, Schmitz JE,
816 Hadjifrangiskou M, Foti A, Dahl J-U. 2022. Redox-Mediated Inactivation of the
817 Transcriptional Repressor RcrR is Responsible for Uropathogenic Escherichia coli's
818 Increased Resistance to Reactive Chlorine Species. mBio 13:e01926-22.
819 40. Kitagawa M, Matsumura Y, Tsuchido T. 2000. Small heat shock proteins, IbpA and
820 IbpB, are involved in resistances to heat and superoxide stresses in Escherichia coli.
821 FEMS Microbiol Lett 184:165–171.
822 41. Lewis K. 2000. Programmed Death in Bacteria. Microbiol Mol Biol Rev 64:503–514.

42. Keyer K, Imlay JA. 1996. Superoxide accelerates DNA damage by elevating free-iron levels. Proceedings of the National Academy of Sciences of the United States of America 93:13635–13640.

43. Liochev SI, Fridovich I. 1994. The role of O2.- in the production of HO.: in vitro and in vivo. Free Radic Biol Med 16:29–33.

44. Taber HW, Mueller JP, Miller PF, Arrow AS. 1987. Bacterial uptake of aminoglycoside antibiotics. Microbiological Reviews 51:439–457.

45. Kim W, Zhu W, Hendricks GL, Van Tyne D, Steele AD, Keohane CE, Fricke N, Conery AL, Shen S, Pan W, Lee K, Rajamuthiah R, Fuchs BB, Vlahovska PM, Wuest WM, Gilmore MS, Gao H, Ausubel FM, Mylonakis E. 2018. A new class of synthetic retinoid antibiotics effective against bacterial persisters. Nature 2018 556:7699 556:103–107.

46. Pletzer D, Mansour SC, Hancock REW. 2018. Synergy between conventional antibiotics and anti-biofilm peptides in a murine, sub-cutaneous abscess model caused by recalcitrant ESKAPE pathogens. PLOS Pathogens 14:e1007084.

47. MacNair CR, Stokes JM, Carfrae LA, Fiebig-Comyn AA, Coombes BK, Mulvey MR, Brown ED. 2018. Overcoming mcr-1 mediated colistin resistance with colistin in combination with other antibiotics. Nature Communications 2018 9:1 9:1–8.

48. Arndt-Jovin DJ, Jovin TM. 1989. Chapter 16 Fluorescence Labeling and Microscopy of DNA. Methods in Cell Biology 30:417–448.

49. Bryan LE, Van Den Elzen HM. 1976. Streptomycin accumulation in susceptible and resistant strains of Escherichia coli and Pseudomonas aeruginosa. Antimicrobial agents and chemotherapy 9:928–938.

50. Nowack B, Krug HF, Height M. 2011. 120 years of nanosilver history: implications for policy makers. Environ Sci Technol 45:1177–1183.

51. Jung WK, Koo HC, Kim KW, Shin S, Kim SH, Park YH. 2008. Antibacterial Activity and Mechanism of Action of the Silver Ion in Staphylococcus aureus and Escherichia coli. Applied and Environmental Microbiology 74:2171–2178.

52. Wakshlak RB-K, Pedahzur R, Avnir D. 2015. Antibacterial activity of silver-killed bacteria: the “zombies” effect. 1. Sci Rep 5:9555.

53. Panáček A, Kvítek L, Smékalová M, Večeřová R, Kolář M, Röderová M, Dyčka F, Šebela M, Prucek R, Tomanec O, Zbořil R. 2017. Bacterial resistance to silver nanoparticles and how to overcome it. Nature Nanotechnology 2017 13:1 13:65–71.

54. Wang H, Wang M, Xu X, Gao P, Xu Z, Zhang Q, Li H, Yan A, Kao RYT, Sun H. 2021. Multi-target mode of action of silver against Staphylococcus aureus endows it with capability to combat antibiotic resistance. Nature Communications 2021 12:1 12:1–16.

55. Tambosi R, Liotenberg S, Bourbon M-L, Steunou A-S, Babot M, Durand A, Kebaili N, Ouchane S. 2018. Silver and Copper Acute Effects on Membrane Proteins and Impact on Photosynthetic and Respiratory Complexes in Bacteria. mBio 9:e01535-18.

56. Vaishampayan A, de Jong A, Wight DJ, Kok J, Grohmann E. 2018. A novel antimicrobial coating represses biofilm and virulence-related genes in methicillin-resistant Staphylococcus aureus. Frontiers in Microbiology 9:1–14.

57. Dwyer DJ, Belenky PA, Yang JH, Cody MacDonald I, Martell JD, Takahashi N, Chan CTY, Lobritz MA, Braff D, Schwarz EG, Ye JD, Pati M, Vercruysse M, Ralifo PS,

869 Allison KR, Khalil AS, Ting AY, Walker GC, Collins JJ. 2014. Antibiotics induce
870 redox-related physi. Proceedings of the National Academy of Sciences of the United
871 States of America 111:E2100–E2109.
872 58. Herisse M, Duverger Y, Martin-Verstraete I, Barras F, Ezraty B. 2017. Silver
873 potentiates aminoglycoside toxicity by enhancing their uptake. Molecular
874 Microbiology 105:115–126.
875 59. Ling J, Cho C, Guo L-T, Aerni H, Rinehart J, Söll D. 2012. Protein aggregation
876 caused by aminoglycoside action is prevented by a hydrogen peroxide scavenger.
877 Mol Cell 48:713–722.
878 60. Ye J, Su Y, Lin X, Lai S, Li W, Ali F, Zheng J, Peng B. 2018. Alanine Enhances
879 Aminoglycosides-Induced ROS Production as Revealed by Proteomic Analysis.
880 Frontiers in Microbiology 9.
881 61. Ji X, Zou J, Peng H, Stolle A-S, Xie R, Zhang H, Peng B, Mekalanos JJ, Zheng J.
882 2019. Alarmone Ap4A is elevated by aminoglycoside antibiotics and enhances their
883 bactericidal activity. Proceedings of the National Academy of Sciences 116:9578–
884 9585.
885 62. Imlay JA. 2002. How oxygen damages microbes: Oxygen tolerance and obligate
886 anaerobiosisAdvances in Microbial Physiology.
887 63. Park S, You X, Imlay JA. 2005. Substantial DNA damage from submicromolar
888 intracellular hydrogen peroxide detected in Hpx- mutants of Escherichia coli.
889 Proceedings of the National Academy of Sciences 102:9317–9322.
890 64. Poole K. 2011. Pseudomonas aeruginosa: Resistance to the max. Frontiers in
891 Microbiology 2:65.

892 65. Hancock REW, Farmer SW, Li Z, Poole K. 1991. Interaction of aminoglycosides with
893 the outer membranes and purified lipopolysaccharide and OmpF porin of Escherichia
894 coli. Antimicrobial Agents and Chemotherapy 35:1309–1314.
895 66. Hancock RE, Raffle VJ, Nicas TI. 1981. Involvement of the outer membrane in
896 gentamicin and streptomycin uptake and killing in Pseudomonas aeruginosa.
897 Antimicrobial Agents and Chemotherapy 19:777–785.
898 67. Wright GD. 2016. Antibiotic Adjuvants: Rescuing Antibiotics from Resistance. Trends
899 in Microbiology 24:862–871.
900 68. Price M, Reiners JJ, Santiago AM, Kessel D. 2009. Monitoring Singlet Oxygen and
901 Hydroxyl Radical Formation with Fluorescent Probes During Photodynamic Therapy.
902 Photochemistry and Photobiology 85:1177–1181.
903 69. Pfaffl MW. 2001. A new mathematical model for relative quantification in real-time
904 RT–PCR. Nucleic Acids Research 29:e45.
905 70. Helander IM, Mattila-Sandholm T. 2000. Fluorometric assessment of Gram-negative
906 bacterial permeabilization. Journal of Applied Microbiology 88:213–219.
907 71. Sabnis A, Hagart KLH, Klöckner A, Becce M, Evans LE, Furniss RCD, Mavridou DAI,
908 Murphy R, Stevens MM, Davies JC, Larrouy-Maumus GJ, Clarke TB, Edwards AM.
909 2021. Colistin kills bacteria by targeting lipopolysaccharide in the cytoplasmic
910 membrane. eLife 10.
911 72. Saito H, Inui K, Hori R. 1986. Mechanisms of gentamicin transport in kidney epithelial
912 cell line (LLC-PK1). Journal of Pharmacology and Experimental Therapeutics 238.
913
914

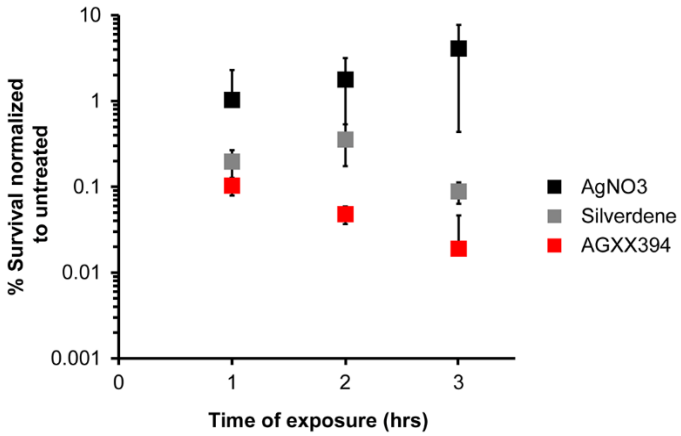

915

916 **FIG 1 AGXX394 is more efficient in killing *P. aeruginosa* than silverdene and silver**
917 **nitrate.** Overnight PA14 cultures were diluted ~25-fold into MOPSg media (OD_{600}=0.1)
918 and treated for three hours with 25 µg/ml $AgNO_3$ (black), silverdene (grey), and AGXX394
919 (red), respectively. Colony survival was evaluated every hour by serially diluting samples
920 and plating them onto LB agar. Percent survival was calculated relative to the untreated
921 control (*n=4, ± S.D)*.

922

923

924

925

926

927

928

929

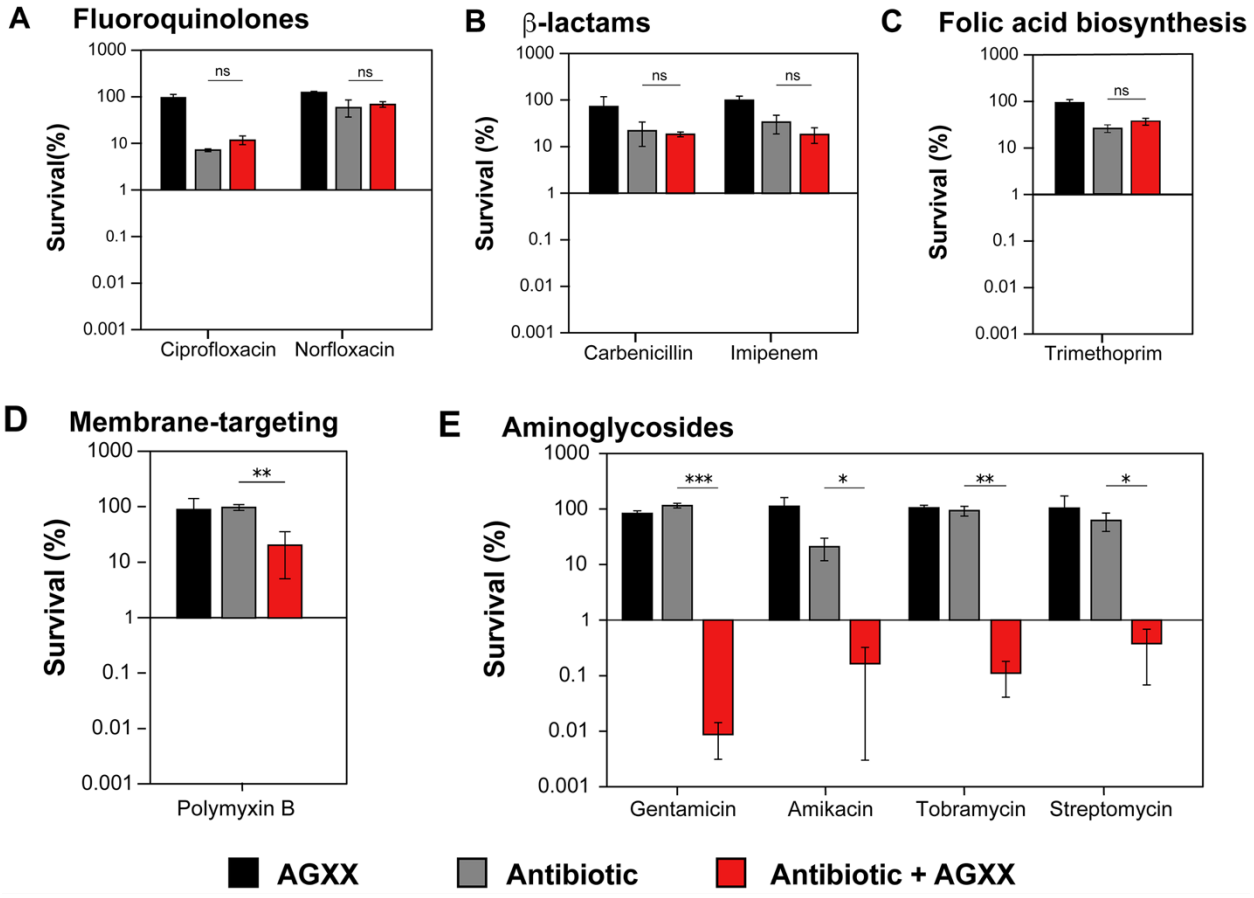

FIG 2 AGXX exponentially increases the activity of aminoglycosides against *P. aeruginosa*. Overnight PA14 cultures were diluted ~25-fold (OD_{600}=0.1) into Mueller-Hinton media and exposed to 75 µg/ml AGXX720C (black bars), a sublethal concentration of the indicated antibiotic (grey bar), or the combined treatment of both (red bars) for 3 hours. Samples were taking every 60 min, serial diluted, plated on LB agar, and incubated for 20 hours for CFU counts. Percent survival was calculated relative to the untreated control for: **(A)** 35 ng/ml ciprofloxacin and 100 ng/ml nalidixic acid, respectively; **(B)** 79 µg/ml carbenicillin and 0.156 µg/ml imipenem, respectively; **(C)** 125 µg/ml trimethoprim; **(D)** 1.5 µg/ml polymyxin B; and **(E)** 0.4 µg/ml gentamicin, 2.0 µg/ml amikacin, 1.0 µg/ml tobramycin, and 3 µg/ml streptomycin, respectively. All experiments were performed in at least three biological replicates and error bars represent mean ± SD. * $p < 0.05$, ** $p < 0.01$, *** $p < 0.001$ (Student's t test, calculated relative to cultures treated with antibiotics alone).

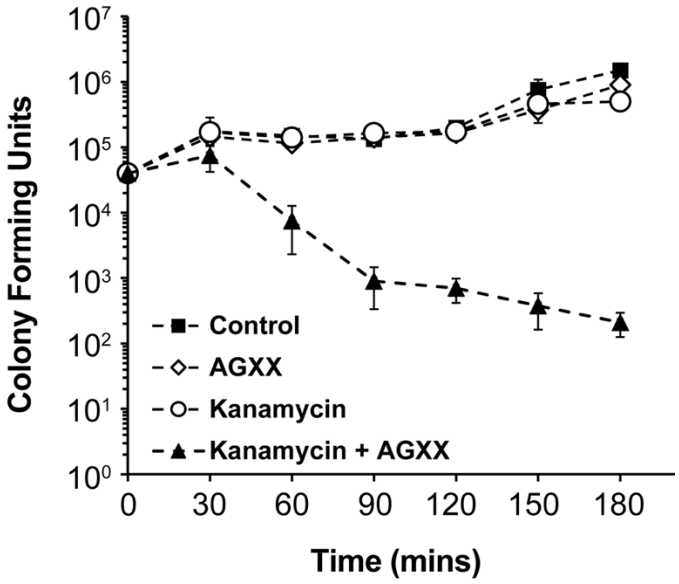

FIG 3 AGXX increases the sensitivity of *P. aeruginosa* strain PA14 to kanamycin. Overnight PA14 cultures were diluted ~25-fold into Mueller-Hinton media (OD_{600}=0.1) and either left untreated or exposed to 75 µg/ml AGXX720C, 50 µg/ml kanamycin, or the combination thereof for 3 hours. Samples were taken every 30 minutes, serial diluted and plated on LB agar for CFU counts, (*n=4, ± S.D)*.

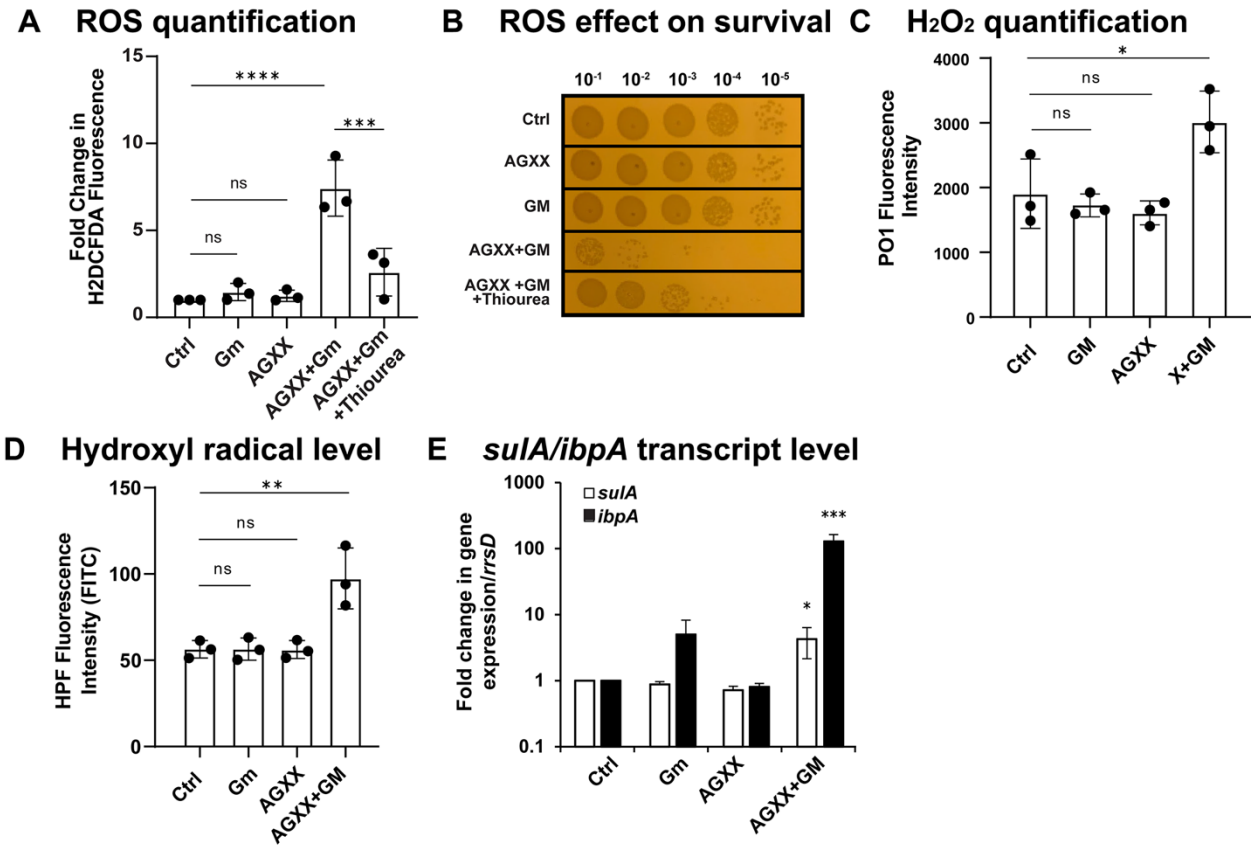

FIG 4 The combination of sublethal concentrations of AGXX and aminoglycosides increases ROS formation and causes DNA damage and protein aggregation. Mid-log PA14 cells were treated with sublethal concentrations of Gm (0.25 µg/ml), AGXX720C (50 µg/ml), the combination thereof, or left untreated. **(A)** Intracellular ROS levels were quantified by H_2DCFDA fluorescence. 50mM thiourea was used as a ROS quencher (*n=3, ± S.D)*. **(B)** Samples were serially diluted in PBS after 60 min of incubation, spot-titered onto LB agar and incubated for 20 hours. One representative of three independent experiments with similar outcomes. **(C, D)** Cells were strained with **(C)** 10 µM peroxy-orange 1 (PO1) and **(D)** 10µM hydroxyphenyl fluorescein (HPF) for 60 min and fluorescence was measured via flow cytometry (*n=3, ± S.D)*. **(E)** The induction of *sulA* (white bar) and *ibpA* (black bar) transcript levels was determined by qRT-PCR. Gene expression was normalized to the housekeeping gene *rrsD* and calculated as fold changes based on expression levels in the untreated control (*n=3, ± S.D.*). One-way ANOVA, Dunnett's posttest; *ns p>0.05,* * $p < 0.05$, ** $p < 0.01$, *** $p < 0.001$, **** $p < 0.0001$.

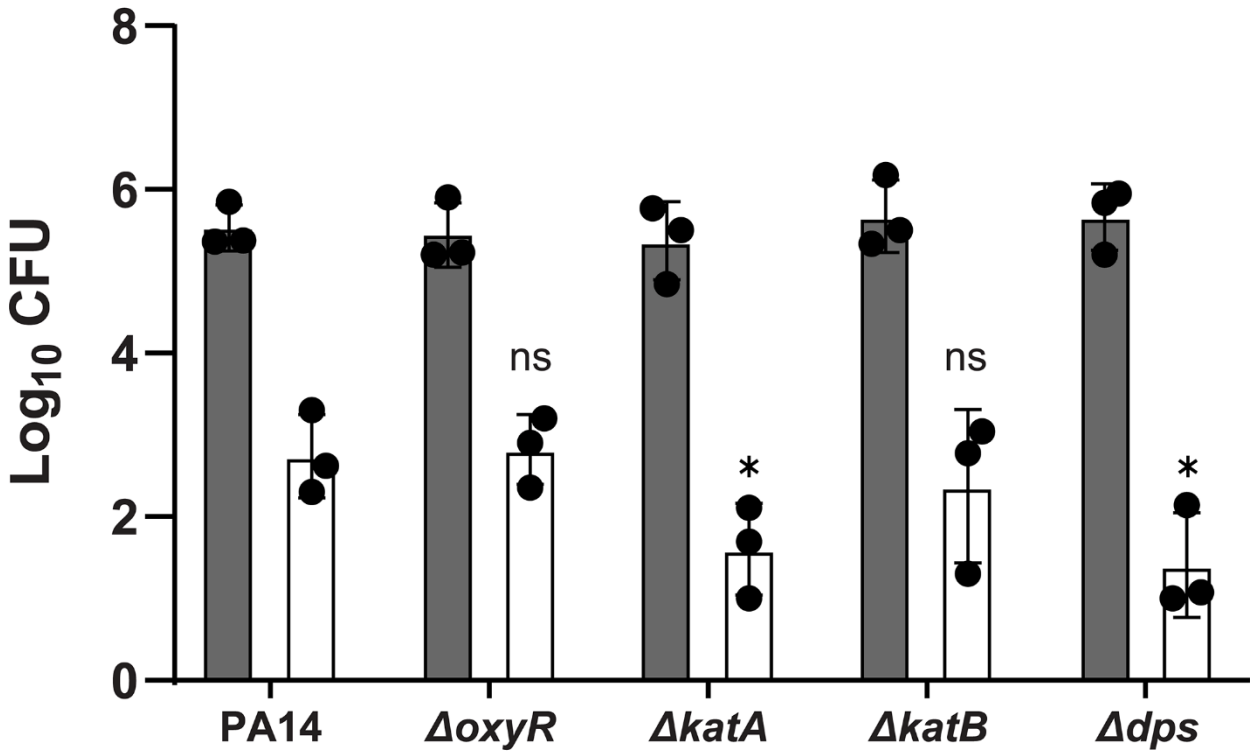

FIG 5 Antioxidant systems provide protection against ROS-mediated damage caused by a combinational treatment of AGXX and aminoglycosides. Overnight cultures of PA14 wildtype, Δ*oxyR,* Δ*katA,* Δ*katB* and Δ*dps* were diluted into MOPSg to an OD_{600}=0.01 and grown under aerobic conditions until OD_{600}=0.1. Cultures were either left untreated (grey bars) or treated with a combination of 0.25 µg/ml tobramycin and 25 µg/ml AGXX720C (white bars). Bacterial survival was quantified after two hours by serially diluting cells in PBS and plating on LB agar for 20 hours at 37°C (*n=3, ± S.D*). Student t-test, * $p < 0.05$).

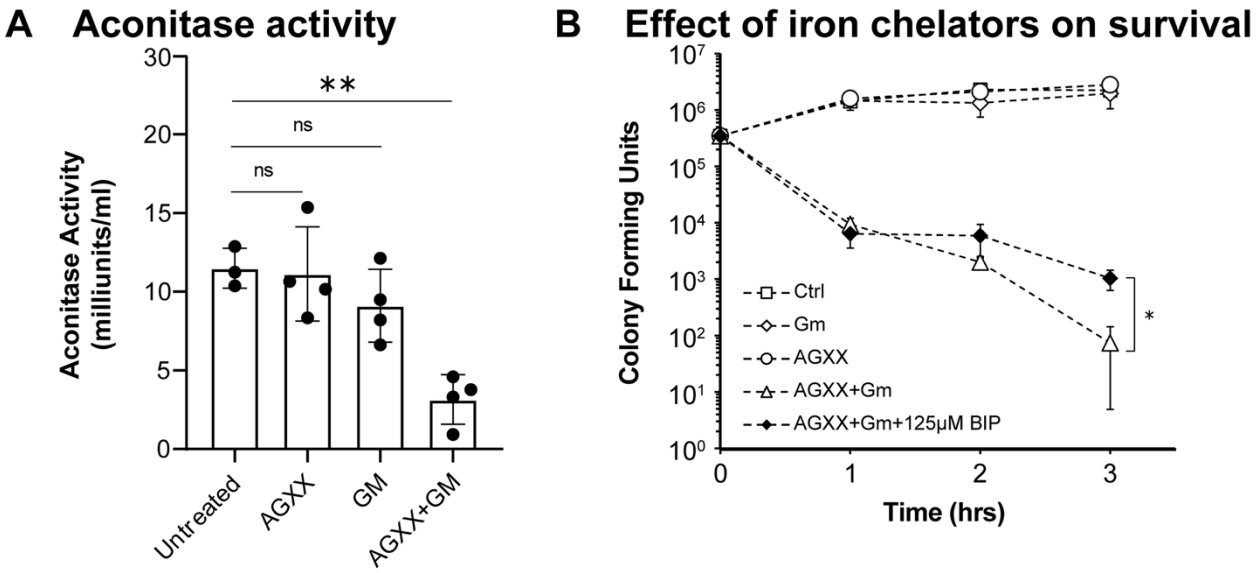

FIG 6 The synergy between AGXX and aminoglycosides on PA14 killing is in parts mediated by a disruption in iron homeostasis. Overnight PA14 cultures were diluted into MOPSg and incubated under aerobic conditions until exponential phase was reached. **(A)** Cells were left untreated or treated with 100 µg/ml AGXX720C, 0.6 µg/ml Gm, or the combination thereof for 1 hour. Aconitase activities were determined in crude extracts (*n=4,* ± *S.D*). One-way ANOVA, Dunnett's posttest; *ns p>0.05,* ** $p < 0.01$. **(B)** Cultures were either left untreated (white square) or treated with 0.25 µg/ml Gm (white diamond), 50µg/ml AGXX720C (white circle), or the combination thereof (white triangle) for three hours. Survival was determined each hour by serially diluting samples in PBS and plating onto LB agar for overnight growth. The impact of free iron on the increased killing by AGXX/Gm cotreatments was tested by the absence (white triangle) and presence (black diamonds) of 125 µM 2',2' bipyridyl (*n=3,* ± *S.D.*). Student's t test, * $p<0.05$).

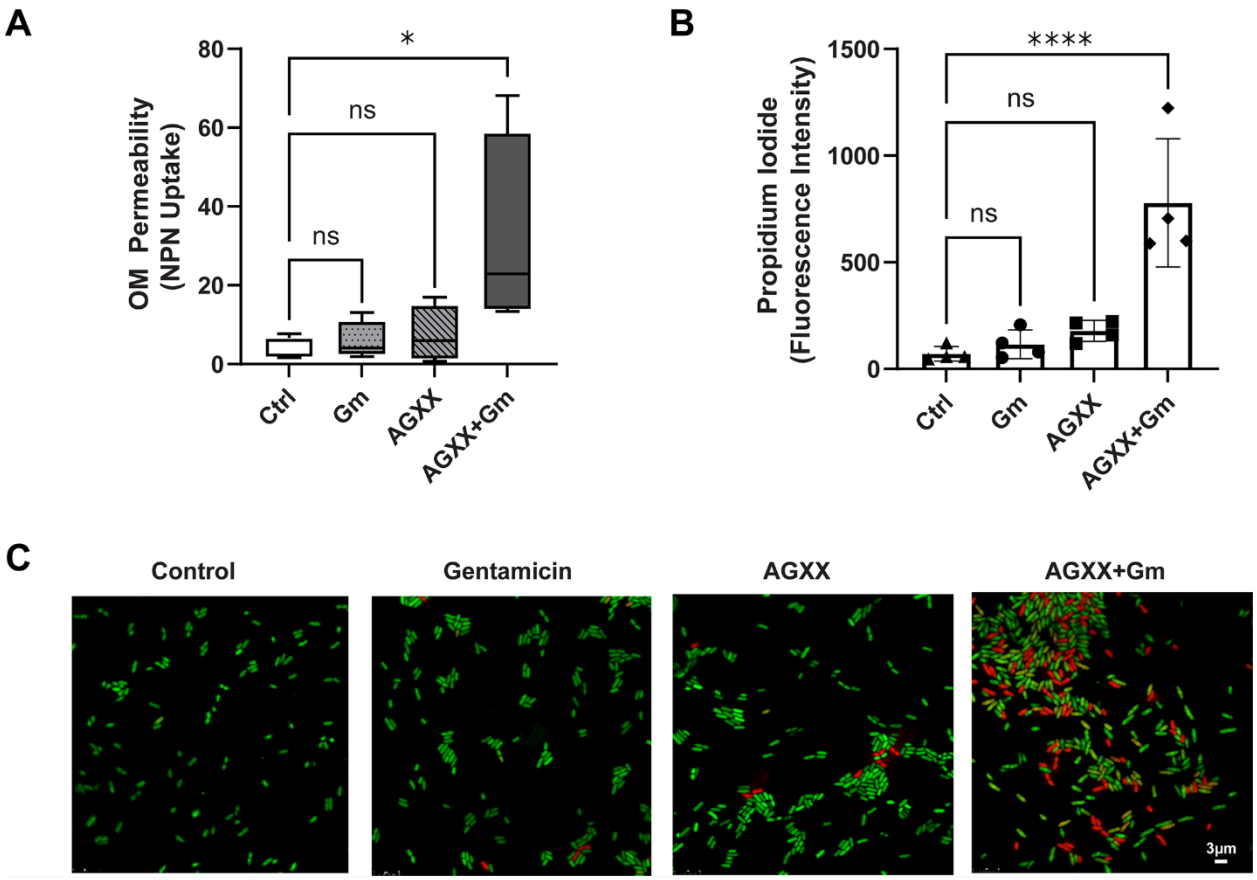

FIG 7 Combined AGXX and aminoglycoside treatment induces significant membrane damage. PA14 cells grown to mid-log phase in MOPSg media were left untreated or treated with sublethal concentrations of Gm (0.25 µg/ml), AGXX720C (50µg/ml), and the combination thereof. Cells were harvested after 1 hour of treatment, washed in PBS, and stained with **(A)** 10 µM N-phenyl-1-naphthylamine (NPN) dye, and **(B)** 0.5 µM propidium iodide (PI). Fluorescence intensities were determined at excitation/emission wavelengths of **(A)** 350/420 nm and **(B)** 535/617 nm, respectively, (*n=4,* ± *S.D.*). One-way ANOVA, Dunnett's posttest; *ns p>0.05,* * $p < 0.05$, **** $p < 0.0001$. **(C)** Samples were washed in PBS, stained with PI/Syto9, incubated in the dark for 15 minutes at room temperature, mounted onto a glass slide with 1% agarose, and imaged at 60x magnification via inverted confocal microscopy. One representative of three independent experiments with similar outcomes.

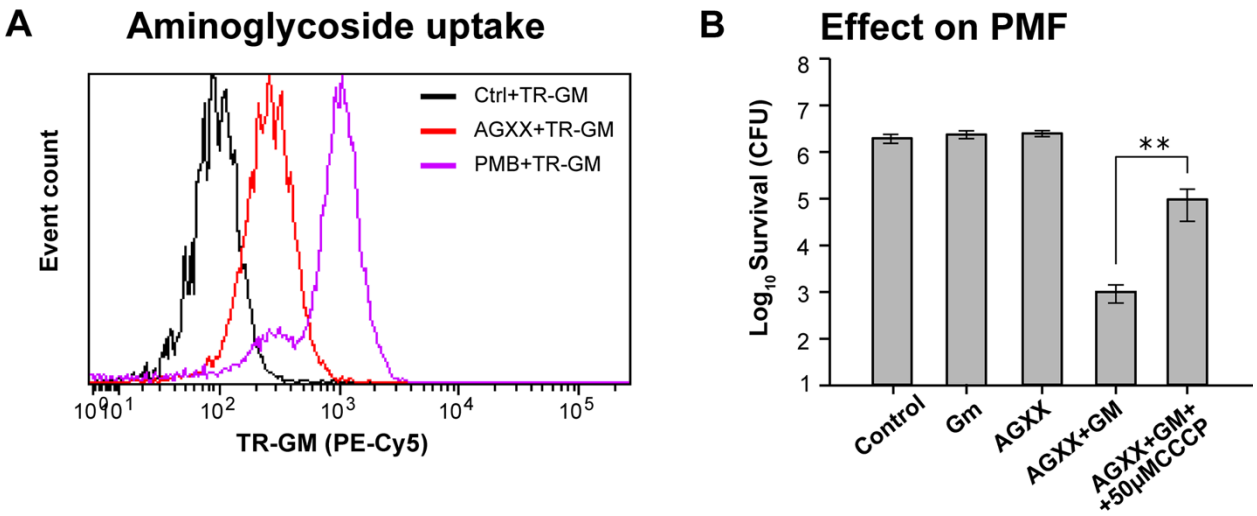

FIG 8 AGXX increases aminoglycoside uptake and lethality through increased activity of the proton motive force (PMF). (A) Mid-log PA14 cells were treated with 1.0 μg/ml TR-Gm, 1.0 μg/ml TR-Gm + 50 μg/ml AGXX720C, and 1.0 μg/ml TR-Gm + 2.0 μg/ml polymyxin B (PMB) for 1 hour, respectively. TR-Gm uptake was measured via flow cytometry. **(B)** Mid-log phase PA14 were left untreated (control) or exposed to 0.25 μg/ml Gm, 50 μg/ml AGXX720C or 0.25 μg/ml Gm + 50 μg/ml AGXX720C for 3 hours. Samples were serial diluted, plated on LB agar, and incubated for 20 hours for CFU counts. To test the impact of the PMF on the killing of a combination of AGXX and aminoglycosides, PA14 were pretreated with or without 50 μM carbonyl cyanide *m*-chlorophenyl hydrazone (CCCP) prior to AGXX/Gm exposure *(n=3, ± S.D.)*. Student's t test, ** $p<0.01$.

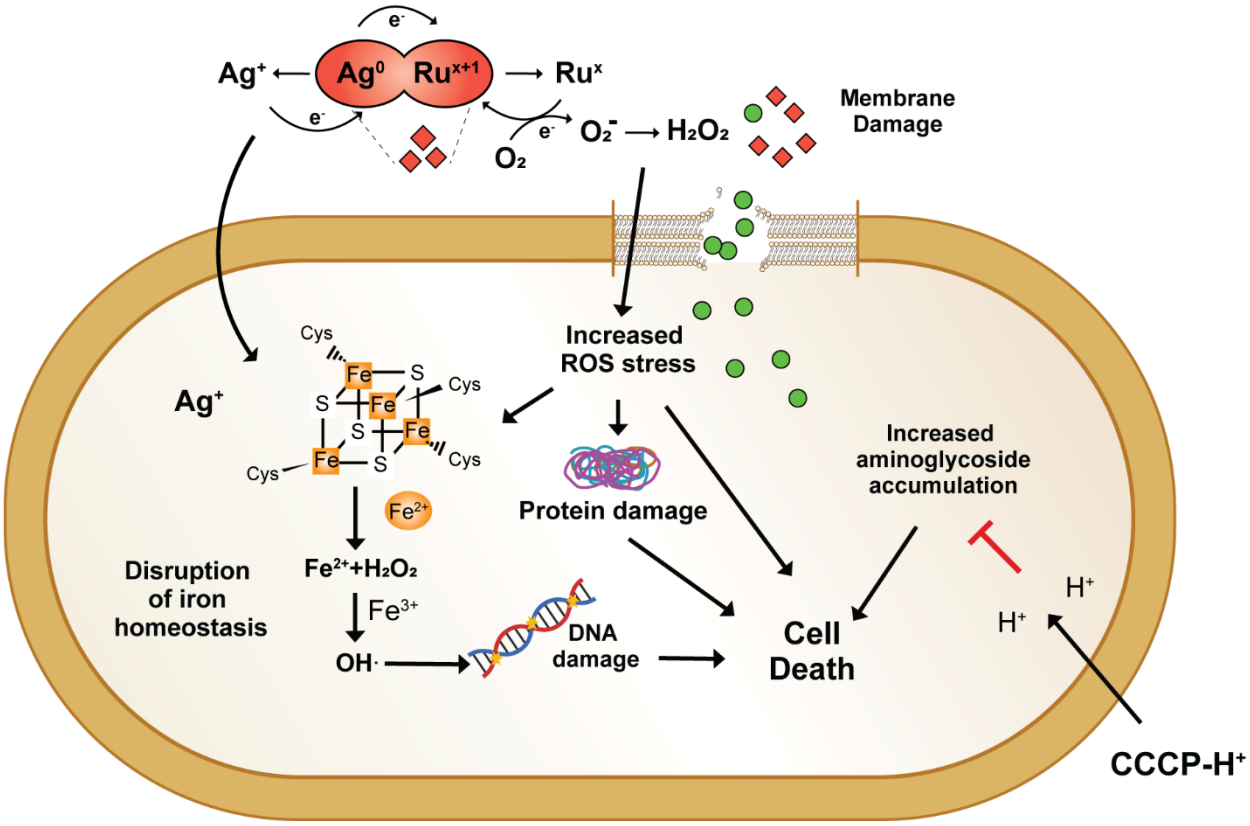

FIG 9 Proposed model for the synergy between AGXX and aminoglycoside antibiotics. The antimicrobial action of AGXX is mediated by superoxide (O_2^-) and hydrogen peroxide (H_2O_2), which are generated in a redox cycle between silver (Ag) and ruthenium (Ru^{x+1}). The combination of AGXX and aminoglycosides concertedly increases endogenous ROS levels. Potentially facilitated by a release of silver ions, the increased ROS level may disrupt iron-sulfur clusters in metabolic enzymes such as aconitase, resulting in the release of free iron, which ultimately triggers hydroxyl radical (OH•) formation in a Fenton reaction. Increasing ROS levels can inflict macromolecule damage such as DNA damage and protein aggregation, contributing to increased killing as observed for *P. aeruginosa* that were treated with a combination of AGXX and aminoglycosides. The synergistic effect between AGXX and aminoglycosides is also mediated by an increased uptake and the cellular accumulation of aminoglycosides, which can be attenuated by disrupting the bacterial membrane potential with ionophores such as CCCP.

Supplementary Information

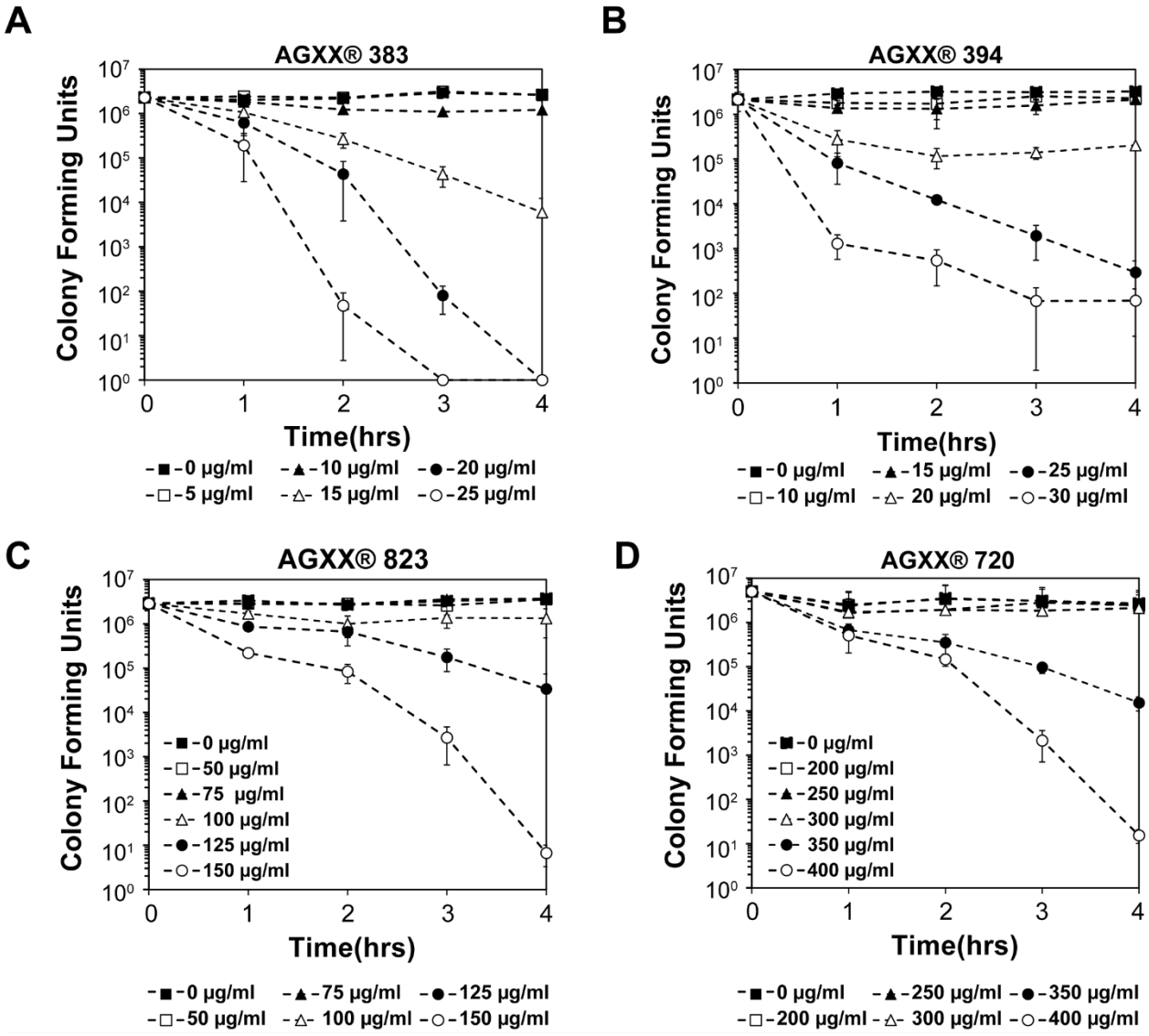

FIG S1 PA14 cultures grown overnight in LB media were diluted 25-fold into MOPSg media and either left untreated (black square) or exposed to the indicated concentrations of **(A)** AGXX383, **(B)** AGXX394, **(C)** AGXX823, and **(D)** AGXX720C, respectively. For the course of four hours, samples were taken every 60 min, serial diluted, plated on LB agar, and incubated for 20 hours for CFU counts (*n=3, ± S.D.).*

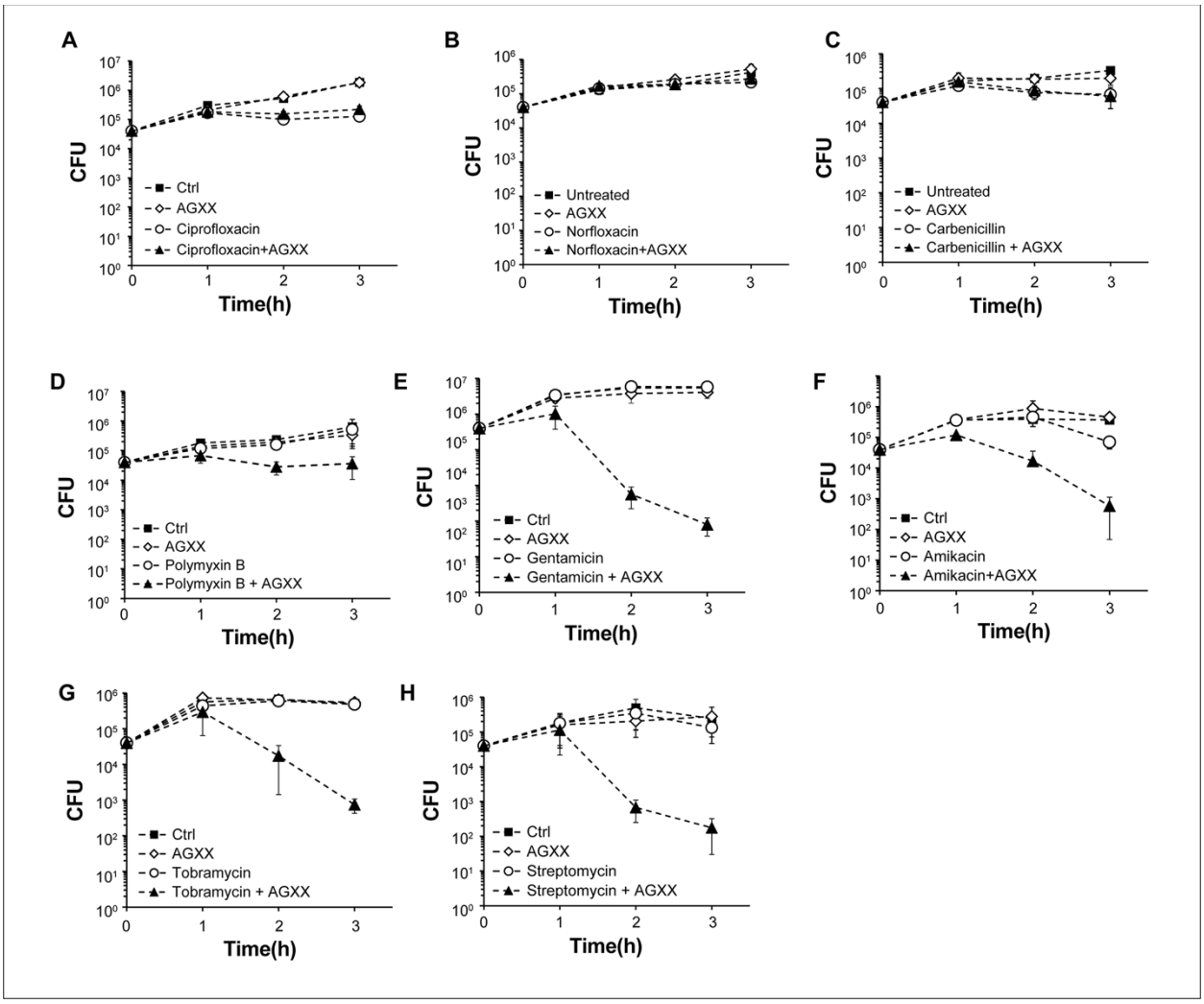

FIG S2 PA14 cultures grown overnight in LB media were diluted ~25-fold (OD_{600}=0.1) into Mueller-Hinton media and either left untreated (black square) or exposed to 75µg/ml AGXX720C (white diamond), a sublethal concentration of the indicated antibiotic (white circle), or the combination thereof (black triangle). For course of 3 hours, samples were taken every 60 min, serial diluted, plated on LB agar, and incubated for 20 hours for CFU counts (*n=3, ± S.D.).* Student's t test, ns p>0.05, * p<0.05, **** p<0.0001).

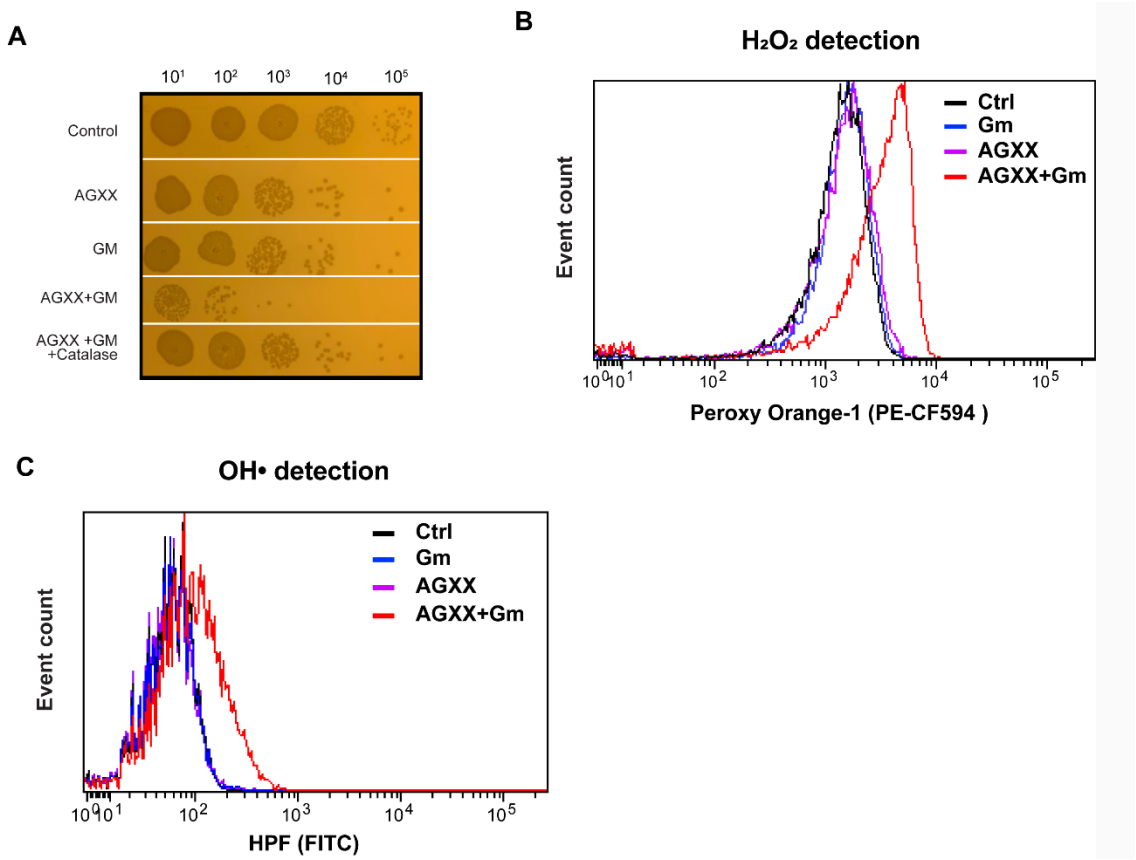

FIG S3 Combined treatment with AGXX and gentamicin increases endogenous ROS levels. (A) Mid-log PA14 cells were treated with sublethal concentrations of Gm (0.25 µg/ml), AGXX720C (50 µg/ml), the combination thereof, or left untreated. Pre-exposure to catalase was used as a ROS quencher. Samples were serially diluted in PBS after 60 min of incubation, spot-titered onto LB agar and incubated for 20 hours. One representative of three independent experiments with similar outcomes. **(B, C)** Exponentially growing PA14 cells were either left untreated or treated with sublethal concentrations of Gm (0.5 µg/ml), AGXX720C (50 µg/ml), and the combination thereof for 60 minutes. Intracellular ROS levels were quantified by staining PA14 cells with **(B)** 10 µM PO1 and **(C)** 10 µM HPF, respectively. Dye fluorescence was measured via flow cytometry after 30 min of incubation. One representative of three independent experiments of similar outcomes.

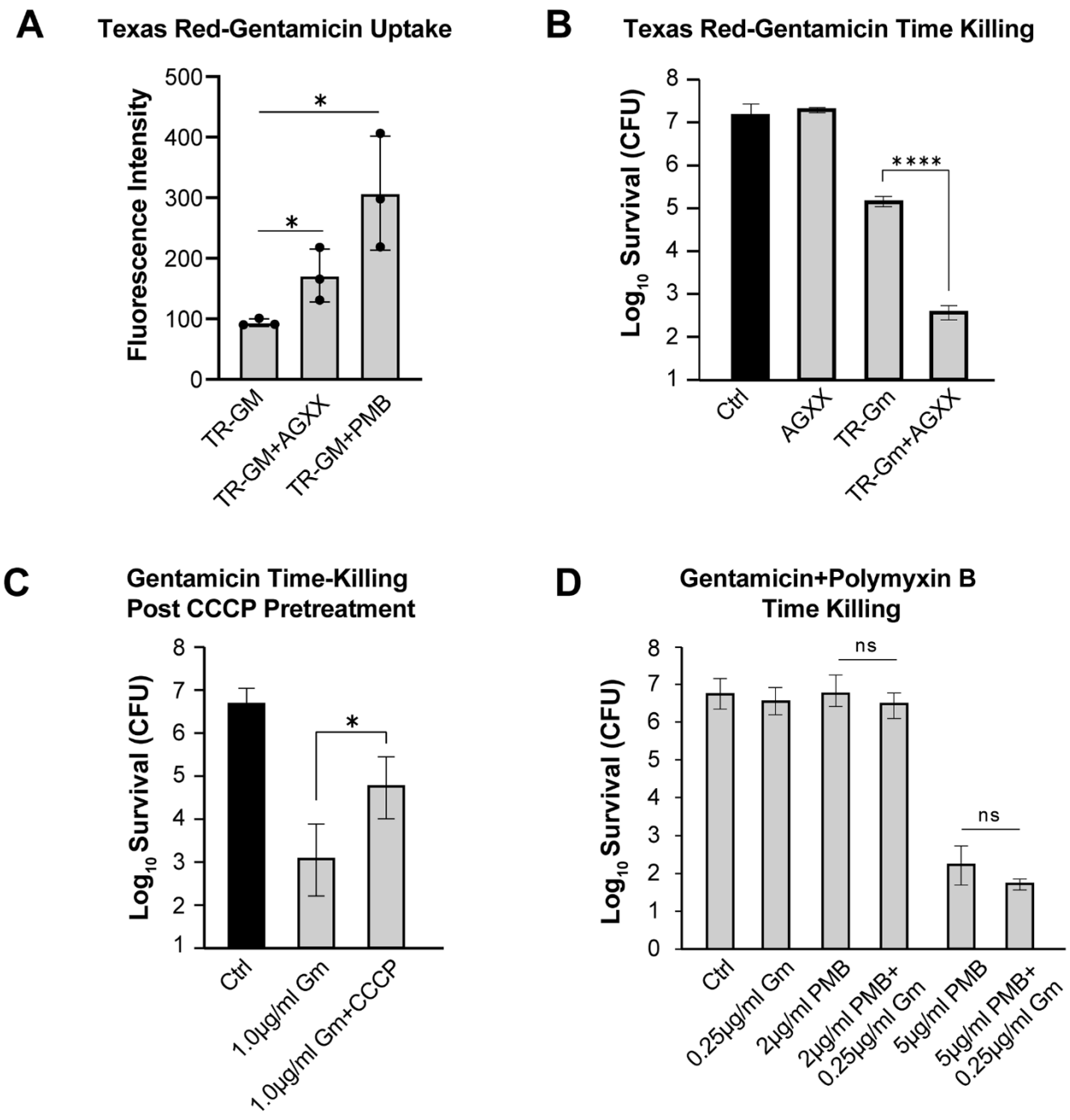

FIG S4 AGXX increases aminoglycoside uptake and lethality through increased PMF activity. PA14 cells were grown to mid-log phase (OD_{600}=0.3) and treated with: **(A)** 1.0 μg/ml TR-Gm in the presence and absence of 50 μg/ml AGXX720C and 2.0 μg/ml polymyxin B, respectively, to measure TR-Gm uptake by flow cytometry after 1 hour of treatment (*n=3, ± S.D.,)*; (**B**) 50 μg/ml AGXX720C, and 1.0 μg/ml TR-Gm in the presence and absence of 50 μg/ml AGXX720C. Samples were taken after 2 hours, serial diluted and plated on LB agar. CFU were counted after 20 hours (*n=3, ± S.D.);* **(C)** To test the

impact of the PMF on the killing of 1 µg/ml Gm, cells were pre-treated with 10 µM carbonyl cyanide *m*-chlorophenyl hydrazone (CCCP) prior to Gm exposure (*n=3, ± S.D.)*; (**D**) polymyxin B (2µg/ml and 5µg/ml, respectively) with or without 0.25 µg/ml Gm for 3 hours. Samples were serial diluted, plated on LB agar, and incubated for 20 hours for CFU counts (*n=3, ± S.D.)*. (Student's t test, ns p>0.05, * p<0.05, **** p<0.0001).